Pharyngeal Immunity in Early Vertebrates Provides Functional and Evolutionary Insight into Mucosal Homeostasis

Wei-guang Kong,*,[1] Yong-yao Yu,*,[1] Shuai Dong,* Zhen-yu Huang,* Li-guo Ding,* Jia-feng Cao,* Fen Dong,* Xiao-ting Zhang,* Xia Liu,* Hao-yue Xu,* Kai-feng Meng,* Jian-guo Su,* and Zhen Xu*,†

The pharyngeal organ is located at the crossroad of the respiratory and digestive tracts in vertebrate, and it is continuously challenged by varying Ags during breathing and feeding. In mammals, the pharyngeal mucosa (PM) is a critical first line of defense. However, the evolutionary origins and ancient roles of immune defense and microbiota homeostasis of PM are still unknown. In this study, to our knowledge, we are the first to find that diffuse MALT is present in PM of rainbow trout, an early vertebrate. Importantly, following parasitic infection, we detect that strong parasite-specific mucosal IgT and dominant proliferation of IgT$^+$ B cell immune responses occurs in trout PM, providing, to our knowledge, the first demonstration of local mucosal Ig responses against pathogens in pharyngeal organ of a nonmammal species. Moreover, we show that the trout PM microbiota is prevalently coated with secretory IgT and, to a much lesser degree, by IgM and IgD, suggesting the key role of mucosal Igs in the immune exclusion of teleost pharyngeal bacteria. Overall, to our knowledge, our findings provide the first evidence that pharyngeal mucosal immunity appear earlier than tetrapods. *The Journal of Immunology*, **2019, 203: 3054–3067.**

The pharynx represents the intersection between the digestive and respiratory tracts in vertebrates (1), and the pharyngeal cavity (PC), for breathing and swallowing, is at risk for vast amounts of microbiota and foreign Ags from air, water, or food (2, 3). In terrestrial vertebrates, a unique choana connects the nasal cavity (NC) and PC (4, 5) and thus makes nasal and pharyngeal lymphoid tissue defined together as nasopharynx-associated lymphoid tissue (NALT), which acts as the first line of defense against external threats (6, 7). In mammals except rodents, NALT consists of organized lymphoid tissues containing adenoids, palatine tonsils, and lingual tonsils with highly organized germinal centers (GCs), known as Waldeyer's ring in humans, as well as a diffuse network of immune cells surround the entrance to the pharynx (8–10). This offers mammals efficient innate and adaptive immunity to protect the upper respiratory tract (11, 12). So far, the pharyngeal tonsil has only been discovered in mammals and birds, whereas no evidence shows that the Waldeyer's ring exists in the pharynx of birds (13, 14). In contrast, cold-blooded animals like reptiles, amphibians, and fish lack tonsils in their PC, and NALT has not been well investigated in these animals (10, 15). Although organized NALT structures in sarcopterygian fish like lungfish are found in the mucosa of the upper and lower jaw, they still lack B and T cell zones and GC formation (16). It is worth noting that teleost NALT has only been described as diffuse NALT in the NC, and it shares the main features of other teleost MALTs, including a dominant role of secreted IgT (sIgT) and IgT$^+$ B cells in mucosal immunity (17, 18). However, because teleost fish lack the choana, and the PC is a separate compartment from the NC, whether MALT appears in the teleost PC remains an enigmatic question.

In aquatic vertebrates like teleost fish, the pharynx morphologically communicates with the gills behind the mouth and above the esophagus. Similar to mammals, teleost PC is also covered with the pharyngeal mucosa (PM), containing two main layers, the stratified squamous epithelium and the collagenous connective tissue (lamina propria [LP]) (19). Interestingly, mammalian PMs are known to contain mucus-producing cells in the epithelial layer as well as the mucus gland in the LP (20, 21), and secreted IgA (sIgA) found in pharyngeal mucus is produced by IgA-producing plasma cells in the PM generated from tonsil GCs (6, 22), which play a crucial role in humoral adaptive immunity in pharyngeal homeostasis (23–25). In contrast to mammals, teleost fish lack the mucus gland, and PM is only populated with abundant mucus

*Department of Aquatic Animal Medicine, College of Fisheries, Huazhong Agricultural University, Wuhan, Hubei 430070, China; and †Laboratory for Marine Biology and Biotechnology, Qingdao National Laboratory for Marine Science and Technology, Qingdao 266071, China

[1]W.-g.K. and Y.-y.Y. contributed equally to this work.

ORCIDs: 0000-0001-7466-6348 (W.-g.K.); 0000-0002-4476-0015 (Y.-y.Y.); 0000-0003-2157-8381 (X.-t.Z.); 0000-0002-9083-0715 (J.-g.S.); 0000-0001-6598-2058 (Z.X.).

Received for publication July 31, 2019. Accepted for publication September 25, 2019.

This work was supported by grants from the National Key Research and Development Program of China (2018YFD0900503 and 2018YFD0900400) (to Z.X.) and the National Natural Science Foundation of China (31873045) (to Z.X.).

The data presented in this article have been submitted to the National Center for Biotechnology Information Sequence Read Archive (https://www.ncbi.nlm.nih.gov/bioproject/PRJNA560631/) under accession number PRJNA560631.

Address correspondence and reprint requests to Prof. Zhen Xu, Department of Aquatic Animal Medicine, College of Fisheries, Huazhong Agricultural University, No. 1, Shizishan Street, Wuhan, Hubei 430070, China. E-mail address: zhenxu@mail.hzau.edu.cn

The online version of this article contains supplemental material.

Abbreviations used in this article: DEG, differentially expressed gene; EdU, 5-ethynyl-2′-deoxyuridine; GC, germinal center; LP, lamina propria; NALT, nasopharynx-associated lymphoid tissue; NC, nasal cavity; pAb, polyclonal Ab; PC, pharyngeal cavity; pIgR, polymeric IgR; PM, pharyngeal mucosa; qPCR, quantitative real-time PCR; RNA-Seq, RNA sequencing; sIgA, secreted IgA; sIgT, secreted IgT; tpIgR, trout polymeric IgR; tSC, secretory component–like molecule.

secreting cells. However, so far, the pharyngeal molecular immunity mechanism within the early bony vertebrates has not been thoroughly investigated. Because teleost fish live in water medium, the PC may be subjected to more stimulation from waterborne Ags and evolutionary selective forces. Hence, we hypothesize that a mucosal immune system is indispensable in the pharynx for protecting the extensive and vulnerable mucosal surface.

Teleost fish represent the most ancient bony vertebrates, containing a specialized mucosal adaptive immune system and secretory Igs (26). So far, three teleost Ig classes (IgM, IgD, and IgT/IgZ) have been identified (27). IgM was thought to be the only functional Ig in teleosts in both the systemic and mucosal compartments. In fact, recent research suggests that IgM immune responses to infection in plasma are stronger than those in mucosal tissues (27, 28). Secreted IgD has been identified in catfish and trout (29, 30), but its function remains enigmatic. In contrast to IgM and IgD, teleost IgT (also called IgZ in some species) is the main mucosal Ig targeting mucosal pathogens and coating microbiota (28, 31–33), akin to IgA in mammals and IgX in amphibians (22, 28). We previously found that IgT is the main mucosal Ig protecting the teleost NC against pathogens (28) and that sIgA plays a major role in the PM of mammals. Thus, despite the independence of the PC from the NC in teleosts, we hypothesize that the role of teleost mucosal Ig in the PC involves a process of convergent evolution between tetrapods and nontetrapods.

To our knowledge, in this study, we are the first to show that the teleost PM is one of ancient MALTs, which can produce strong innate and adaptive immune responses to the infection with parasite *Ichthyophthirius multifiliis*. Moreover, we provide the first demonstration, to our knowledge, that sIgT is the main player involved in pathogen-specific immune responses. Critically, we show that IgT^+ B cells are locally proliferated and generate parasite-specific IgT in the PM of rainbow trout, thus providing, to our knowledge, the first evidence of locally induced mucosal Igs responses in the PM of early vertebrates. Finally, we discover that teleost IgT plays a crucial role in immune exclusion by coating the symbiotic bacteria on the PM. Overall, our findings reveal that the presence of MALT in the PM of a nontetrapod species and sIgT plays a vital role in protecting the PC from invading pathogens.

Materials and Methods

Ethics statement

All animal procedures were performed in accordance with the recommendations in the Guide for the Care and Use of Laboratory Animals of the Ministry of Science and Technology of China and were approved by the Animal Experiment Committee of Huazhong Agricultural University (permit number HZAUFI-2016-007). All efforts were made to minimize the suffering of the animals.

Fish maintenance

Rainbow trout (mean weight, 200–300 g) used for pharyngeal bacteria isolation and rainbow trout (mean weight, 20–25 g) used in infection trials were obtained from a fish farm in Shiyan (Hubei, China) and maintained in aquarium tanks using a water recirculation system involving thermostatic temperature control and extensive biofiltration. Fish were acclimatized for 14 d at 15°C and fed daily with commercial trout pellets at a rate of 1% body weight per day, and feeding was terminated 48 h prior to sacrifice. Grass carp (*Ctenopharyngodon idellus*), southern catfish (*Silurus meridionalis*), mandarin fish (*Siniperca chuatsi*), and snakehead (*Channa argus*) were purchased from aquatic product market in Wuhan (Hubei, China).

I. multifiliis *parasite isolation and infection*

The method for *I. multifiliis* parasite isolation and infection were used as explained elsewhere (18). Briefly, heavily infected rainbow trout were anesthetized with overdose of MS-222 and transferred to a beaker with water to allow trophonts and tomonts exit the fish. After 4 h, the fish were removed, and the trophonts and tomonts were left in the water at 15°C for 24 h to let tomocyst formation and subsequent theront release. For parasite infection, two types of challenges with *I. multifiliis* parasite were performed. In the first one, fish were exposed by bath with a single dosage of ~5000 theronts per fish for 3 h and then transferred into the aquarium containing new aquatic water. Tissue samples were taken at 0.5, 1, 4, 7, 14, 21, 28 and 75 d, and fluids (serum and pharyngeal mucus) were taken on day 28 (infected group) following *I. multifiliis* challenge. For the second type of challenge, fish were monthly exposed with ~5000 theronts per fish (survivor group) for 3 h at 0, 30, and 60 d and then moved to tanks with clean water after each infection. Tissue samples and fluids (serum and pharyngeal mucus) were taken 15 d after the last challenge. Control fish (control group) were exposed to same tank water but without the parasites.

RNA isolation and quantitative real-time PCR analysis

Total RNA was extracted using TRIzol reagent (Invitrogen) according to the manufacturer's protocol. Tissue was homogenized by TissueLyser II (Jingxin Technology) with 5-mm stainless steel beads (QIAGEN) at 60 Hz for 1 min following the manufacturer's instructions. The quantification and concentration of the extracted RNA was carried out by spectrophotometry (NanoPhotometer NP80 Touch), and the integrity of the RNA was determined by agarose gel electrophoresis. To normalize gene expression levels for each sample, equivalent amounts of total RNA (1000 ng) were used for cDNA synthesis as previously described (18). The synthesized cDNA was diluted four times and then used as a template for quantitative real-time PCR (qPCR) analysis. The qPCRs were performed on a 7500 Real-Time PCR System (Applied Biosystems) using the 2× SYBR Green qPCR Master Mix (YEASEN). All samples were performed in following conditions: 95°C for 5 min, followed by 40 cycles at 95°C for 10 s and at 58°C for 30 s. A sample from the serial dilution was run on a 1% agarose gel and stained with Red Gel Stain and viewed under UV light to confirm a band of the correct size was amplified. Trout elongation factor 1α (EF-1α) was used as control gene for normalization of expression. The relative expression level of the genes was determined using the Pfaffl method (34). The primers used for qPCR are listed in Supplemental Table I.

RNA sequencing library construction, sequencing, and bioinformatical analyses

The RNA sequencing (RNA-Seq) libraries from 12 samples (control fish of day 14; control fish of day 28; day 14 exposed to *I. multifiliis*; day 28 exposed to *I. multifiliis*) were generated similarly as in a previous study (35). Briefly, polyadenylated RNA fragments were purified by a Dynabeads mRNA Purification Kit, fragmented with RNA fragmentation buffer, and reverse transcribed into first-strand cDNA using random hexamer and SuperScript II Reverse Transcriptase, followed by second-strand cDNA synthesis using RNase H and DNA polymerase I. The resulting cDNA was end repaired, and a single "A" was added at the 3′ ends, and a unique identifier was labeled at the 5′ ends before ligating to Illumina paired-end sequencing adaptors. PCR was amplified using Phusion High-Fidelity Master Mix and Illumina primers with the condition of 98°C for 60 s, 15 cycles of 98°C for 10 s, and 65°C for 75 s and concluding with 65°C for 5 min. All RNA-Seq data were generated by Illumina paired-end sequencing with read length 150 bp. Reads were mapped to the *Oncorhynchus mykiss* genome using STAR (36) with default parameters. The mapped reads were analyzed by feature counts (37). Differential expression was estimated with edgeR package (38). We excluded the genes with low expression (count-per-million fewer than one in three or more samples) from downstream analysis. The resulting genes were considered as differentially expressed genes (DEGs) if false discovery rate ≤ 0.05 and $\log_2$ (fold-change) ≥ 1. To further understand the transcriptomic data, we carried out a gene ontology enrichment using KEGG Orthology-Based Annotation System (39) to determine the biological processes that were significantly upregulated following *I. multifiliis* infection. The National Center for Biotechnology Information Sequence Read Archive accession number for data reported in this manuscript is PRJNA560631 (https://www.ncbi.nlm.nih.gov/bioproject/PRJNA560631/).

Collection of serum, pharyngeal mucus, and pharyngeal bacteria

For sampling, trout were sacrificed with an overdose of MS-222, and serum was collected and stored as described (31). To obtain pharyngeal mucus, we modified the method described previously (33). Briefly, trout pharyngeal tissue was excised rinsed with PBS three times to remove the remaining blood and then incubated for 12 h at 4°C, with slight shaking in protease inhibitor buffer (1×PBS, containing 1× protease inhibitor mixture [Roche], 1 mM PMSF [Sigma-Aldrich] [pH 7.2]) at a ratio of 1 g of pharyngeal tissue per milliliter of buffer. The suspension (including pharyngeal mucus

and bacteria) was collected, vigorously vortexed, and then centrifuged at 400 × *g* for 10 min at 4°C to remove trout cells. To separate pharyngeal bacteria from mucus, the cell-free supernatant was thereafter centrifuged at 10,000 × *g* for 10 min. The resulting supernatant (containing pharyngeal mucus) was harvested, filtered with a 0.45-μm syringe filter (MilliporeSigma), and stored at 4°C prior to use the same day, whereas the pellet (containing pharyngeal bacteria) was washed three times with PBS (pH 7.2) and resuspended for further analysis.

Isolation of trout leukocytes from trout HK and pharyngeal tissue

The leukocytes from head kidney were obtained with 51/34% discontinuous Percoll density gradients as described previously (40). To obtain trout leukocytes from pharyngeal tissue, we modified the protocol from that used to isolate trout skin leukocyte as previously described (32). Briefly, rainbow trout were anesthetized with an overdose of MS-222, and blood was collected from the caudal vein. Pharyngeal tissue was obtained from each fish and washed carefully with cold PBS to avoid blood contamination. Thereafter, the pharyngeal tissue was cut into small pieces and then treated with modified DMEM (DMEM supplemented with 5% FBS, 100 U/ml penicillin, and 100 μg/ml streptomycin) containing 0.15 mg/ml collagenase IV (Invitrogen), for 30 min at 4°C with continuous shaking. The supernatant was collected, and the aforementioned procedure was repeated again. The pharyngeal tissue pieces were mechanically disaggregated on a 100-μm cell shredder, and the cell fraction was collected. Finally, all cell fractions obtained from the pharyngeal tissue after mechanical and enzymatic treatments were pooled and washed three times in fresh modified DMEM and layered over a 51/34% discontinuous Percoll gradient. After 30 min of centrifugation at 400 × *g*, cells lying at the interface of the gradient were collected and washed with modified DMEM medium.

SDS-PAGE and Western blot

Pharyngeal mucus and serum samples were collected as described above and boiled in SDS-PAGE Sample Loading Buffer (CWBiotech) at 95°C for 5 min and then resolved on 4–15% precast polyacrylamide gel (Bio-Rad Laboratories) under nonreducing or reducing conditions. The gels were transferred onto polyvinylidene difluoride membranes (Bio-Rad Laboratories) with Trans-Blot SD (Bio-Rad Laboratories) by semidry method. For Western blot analysis, the membranes were blocked with 8% skim milk and incubated with anti-trout IgT (rabbit polyclonal Ab [pAb], 0.2 μg/ml), anti-trout IgM (mouse mAb, 0.2 μg/ml), or biotinylated anti-trout IgD (mouse mAb, 0.2 μg/ml) Abs or their respective isotypes control (IgG; BD Biosciences), followed by incubation with peroxidase-conjugated anti-rabbit, anti-mouse IgG (Invitrogen) or streptavidin (Invitrogen). For quantitative analyses of IgT, IgM, and IgD in pharyngeal mucus and serum, immunoreactive bands were first visualized with Clarity Western ECL Substrate (Bio-Rad Laboratories) and scanned by Amersham Imager 600 Imaging System (GE Healthcare), and then band densitometry was analyzed with ImageQuant TL software (GE Healthcare). Finally, the concentrations of IgT, IgM, and IgD were determined by plotting the obtained signal strength values on a standard curve generated for each blot using known amounts of purified trout IgT, IgM, or IgD.

The three Abs (anti-trout IgT [rabbit pAb], anti-trout IgM [mouse mAb], or biotinylated anti-trout IgD [mouse mAb]) we used in our experiments are gifted from our cooperative laboratory (Dr. O. Sunyer's laboratory), and the specificities of these Abs have been confirmed in those papers (33).

Gel filtration

To analyze the monomeric or polymeric state of Igs in trout pharyngeal mucus, gel filtration was performed as described previously for gut and gill mucus (31, 33). Briefly, fractions containing the IgM, IgD or IgT were separated by gel filtration using a Superdex 200 FPLC column (GE Healthcare). The column was previously equilibrated with cold PBS (pH 7.2), and protein fractions were eluted at 0.5 ml/min with PBS using a fast 2protein liquid chromatography instrument with purifier systems (GE Healthcare). Identification of IgM, IgD, and IgT in the eluted fractions was performed by Western blot analysis using anti-IgM, anti-IgD, and anti-IgT Abs, respectively, as described above. A standard curve was generated by plotting the elution volume of the standard proteins in a Gel Filtration Standard (Bio-Rad Laboratories) against their known m.w., which was then used to determine the m.w. of the eluted IgT, IgM, and IgD by their elution volume.

Flow cytometry

For flow cytometry analysis, trout leukocytes suspensions were double stained with monoclonal mouse anti-trout IgT and anti-trout IgM (1 μg/ml each) at 4°C for 45 min. After washing three times, PE goat anti-mouse IgG1 and APC goat anti-mouse IgG2b (2 μg/ml each; BD Biosciences) were added and incubated at 4°C for 30 min to detect IgM^+ and IgT^+ B cells, respectively. Samples were washing three times prior to flow cytometric analysis. Pharyngeal bacteria were stained with anti-trout IgM or anti-trout IgT (1 μg/ml each), or their respective isotypes control (1 μg/ml each; BD Biosciences), at 4°C for 2 h with continuous shaking. After washing three times, secondary Abs Alexa Fluor 488 goat anti-mouse IgG1 or Alexa Fluor 488 goat anti-mouse IgG2b (1 μg/ml each; BD Biosciences) were added and incubated for 45 min at 4°C. To discriminate bacteria from debris, pharyngeal bacteria were labeled with BacLight Green Bacterial Stain (Invitrogen), following the manufacturer's instructions. After three times washing, analysis of stained leukocytes and bacteria were analyzed with a CytoFLEX Flow Cytometer (Beckman Coulter) and FlowJo software (Tree Star).

Histology, light microscopy, and immunofluorescence microscopy studies

The pharyngeal tissues of grass carp, southern catfish, mandarin fish, snakehead, and rainbow trout were dissected and processed for routine histology as described previously (18). Briefly, all tissue samples were fixed in 4% neutral buffered formalin (1:10) overnight at 4°C and then transferred to 70% ethanol. Samples were embedded in paraffin and 5-μm sections were stained with H&E. Images were acquired in a microscope (Olympus) using the AxioVision software. For the detection of *I. multifiliis* parasite at the same time of IgT^+ and IgM^+ B cells, we used rabbit anti-trout IgT (0.5 μg/ml) polyclonal Ab and mouse anti-trout IgM (1 μg/ml) mAb to incubate sections overnight at 4°C. For the detection of *I. multifiliis* parasite at the same time of IgT^+ and IgD^+ B cells, we used rabbit anti-trout IgT (0.5 μg/ml) polyclonal Ab and mouse anti-trout IgD (2 μg/ml) mAb to incubated sections overnight at 4°C. After washing three times with PBS, secondary Abs Alexa Fluor 488-conjugated AffiniPure Goat Anti-Rabbit IgG or Cy3-conjugated AffiniPure Goat Anti-Mouse IgG (3 μg/ml each; Jackson ImmunoResearch Laboratories) were added and incubated at temperature for 40 min to detect IgT^+ and IgM^+ or IgT^+ and IgD^+ B cells, respectively. After washing three times with PBS, mouse anti–*I. multifiliis* polyclonal Ab (1 μg/ml) were added and incubated at 4°C for 6 h. After washing three times with PBS, secondary Ab Alexa Fluor 647 Goat anti-mouse (Jackson ImmunoResearch Laboratories) with 5 μg/ml were added and incubated at temperature for 40 min to detect *I. multifiliis* parasite. For the detection of pharyngeal trout polymeric IgR (tpIgR), we used the same methodology described to stain gill tpIgR using our rabbit anti-tpIgR (33). As controls, the rabbit IgG prebleed and the mouse-IgG1 isotype Abs were used at the same concentrations. All sections were stained with DAPI (1 μg/ml; Invitrogen) before mounting with fluorescent microscopy mounting solution. Pharyngeal bacteria were stained as previously described in the above section and stained bacteria were cytospinned on glass slides and mounted with fluorescent microscopy mounting solution. Images were acquired and analyzed using Olympus BX53 fluorescence microscope (Olympus) and the iVision-Mac scientific imaging processing software (Olympus).

Proliferation of B cells in the pharyngeal tissue of trout

For proliferation of B cells in trout, we modified the methodology as previously reported (31, 33). Briefly, survivor and control fish (~30 g) were anesthetized with MS-222 and i.v. injected with 300 μg 5-ethynyl-2′-deoxyuridine (EdU) (Invitrogen) in 150 μl of PBS. After 24 h, leukocytes from pharyngeal tissue or head kidney were obtained as described above, and cells were incubated with mAb mouse anti-trout IgM or anti-trout IgT (1 μg/ml each) on ice for 1 h. After washing three times, Alexa Fluor 488 goat anti-mouse IgG1 or Alexa Fluor 488 goat anti-mouse IgG2b (3 μg/ml each; Invitrogen) were used as secondary Ab to detect IgM^+ or IgT^+ B cells, respectively. After 40 min incubation on ice, cells were washed three times with DMEM medium and fixed. EdU^+ cell detection was performed according to the manufacturer's instructions (Click-iT Plus EdU Alexa Fluor 647 Flow Cytometry Assay Kit; Invitrogen). Cells were then analyzed with a CytoFLEX Flow Cytometer (Beckman Coulter) and FlowJo software (Tree Star). For immunofluorescence analysis, we used rabbit anti-trout IgT (0.5 μg/ml) polyclonal Ab and mouse anti-trout IgM (1 μg/ml) mAb to incubate paraffin sections of pharyngeal tissues from control and survival fish previously injected with EdU overnight at 4°C. After washing with PBS, sections were incubated with Alexa Fluor 488-conjugated AffiniPure Goat anti-rabbit IgG or Cy3-conjugated AffiniPure Goat anti-mouse IgG (3 μg/ml each; Jackson ImmunoResearch Laboratories) for 2 h at room temperature. As primary control Abs, the rabbit prebleed, and the mouse-IgG1 isotype controls were used at the same concentrations. Stained cells were fixed and EdU^+ cell detection

was performed according to the manufacturer's instructions (Click-iT EdU Alexa Fluor 488 Imaging Kit; Invitrogen). All sections were stained with DAPI (1 μg/ml; Invitrogen) before mounting with fluorescent microscopy mounting solution. Images were acquired and analyzed using Olympus BX53 fluorescence microscope (Olympus) and the iVision-Mac scientific imaging processing software (Olympus).

Tissue explants culture

To assess whether the parasite-specific IgT responses were locally generated in the pharyngeal tissue, we analyzed parasite-specific Ig titers from medium derived of cultured pharynx, head kidney, and spleen explants obtained from control and survivor fish, as described previously (31). Briefly, control and survivor fish were sacrificed with an overdose of MS-222, and blood was removed through the caudal vein to minimize the blood content in the collected organs. Thereafter, head kidney, spleen, and pharynx (~30 mg each tissue) were collected and submerged in 70% ethanol for 1 min to eliminate possible bacteria on their surface. After washed twice with PBS, tissues were placed in a 24-well plate and cultured with 300 ml DMEM medium (Life Technologies), supplemented with 10% FBS, 100 U/ml penicillin, 100 μg/ml streptomycin, 200 μg/ml amphotericin B, and 250 μg/ml gentamicin sulfate, with 5% CO_2 at 17°C. After 7 d culture, supernatants were harvested, centrifuged, and stored at 4°C prior to use the same day.

Binding of trout Igs to I. multifiliis

To assess whether infected and survivor fish had generated parasite-specific Igs, the capacity of IgT, IgM, and IgD from serum, pharyngeal mucus, or tissue (pharynx, spleen, and head kidney) explant supernatants to bind to *I. multifiliis* were measured using a pull-down assay as described previously (31, 32). Briefly, parasites (~100 tomonts) were preincubated with a solution of 0.5% BSA in PBS (pH 7.2) at 4°C for 2 h. Subsequently, parasites were incubated with diluted pharyngeal mucus or serum or tissue (pharynx, head kidney, and spleen) explant supernatants from infected, survivor, or control fish overnight at 4°C with continuous shaking in a 300 μl volume. Dilutions were made with PBS containing 0.5% BSA (pH 7.2). After incubation, the tomonts were washed three times with PBS, and bound proteins were eluted with 2× Laemmli Sample Buffer (Bio-Rad Laboratories) and boiled for 5 min at 95°C. The eluted material was resolved on 4–15% SDS-PAGE Ready Gel (Bio-Rad Laboratories) under nonreducing conditions, and the presence of IgT, IgM, or IgD was detected by Western blotting using the anti-trout IgT, IgM, or IgD Abs, as described above.

Coimmunoprecipitate studies

To detect whether polymeric trout IgT present in the pharyngeal mucus was associated to a secretory component-like molecule derived from trout secretory component–like molecule (tSC), we used the same strategy previously described by us to detect the association of tpIgR to IgT in gut, gill, and nasal mucus (18, 31, 33). Briefly, 10 μg of anti-IgT were incubated with 400 μl of trout pharyngeal mucus overnight at 4°C. As negative control for anti-IgT, the rabbit IgG (purified from the prebleed serum of the rabbit) was used at the same concentrations. The 50 μl of Protein G Agarose (Invitrogen) was first washed five times with PBS and added into each reaction mixture and then incubated for 2 h at 4°C. Thereafter, the beads were washed five times with PBS, and subsequently bound proteins were eluted in 2× Laemmli Sample Buffer (Bio-Rad Laboratories). The eluted material was resolved by SDS-PAGE on 4–15% Tris-HCl Gradient Ready Gels (Bio-Rad Laboratories) under reducing (for tSC detection) or nonreducing (for IgT detection) conditions. Western blot was performed with anti-pIgR and anti-IgT Abs as described above.

Statistical analysis

Data were analyzed in Prism version 6.0 (GraphPad Software). An unpaired Student *t* test and one-way ANOVA with Bonferroni correction (Prism version 6.0; GraphPad Software) were used for analysis of differences between groups. Data are expressed as mean ± SEM. All p values <0.05 were considered statistically significant.

Results

Teleost PM shares universal features with teleost MALTs

In this study, we examined the morphological structure of the PM in rainbow trout and found that, similar to the teleost gut, three typical layers are present in the pharynx: 1) mucosa (epithelium, stratum basale, and LP); 2) submucosa; and 3) muscularis propria (Fig. 1A). Interestingly, taste buds were found on top of the papillae of the submucosa (Fig. 1A), as discovered in mammals (41). To understand the histological organization of the teleost PM, we processed the paraffin sections of PM stained with H&E (Fig. 1B, upper) and Alcian blue (Fig. 1B, lower) obtained from five different teleost families: Cyprinidae, Siluridae, Percichthyidae, Channidae, and Salmonidae (Fig. 1B). We observed that the PMs of grass carp (*C. idellus*), southern catfish (*S. meridionalis*), mandarin fish (*S. chuatsi*), snakehead fish (*Ophiocephalus argus* Cantor), and rainbow trout (*O. mykiss*) all harbored abundant lymphoid cells scattered in the pharyngeal epithelium and LP (Fig. 1B, upper) and a large number of mucous cells in the pharyngeal epithelium (Fig. 1B, lower). These results were in agreement with the teleost MALTs (i.e., GALT, skin-associated lymphoid tissue, and NALT). Moreover, to understand the expression of immune-related genes in the PM from the control adult rainbow trout, we measured the levels of expression of 22 immune-related genes and cell markers in mucosal tissues (skin, gut, and gills) and systemic tissues (spleen and head kidney) as well as the PM by reverse transcription qPCR (Fig. 1C). By cluster analysis of the gene expression profiles of six candidate tissues, we found that PM is clustered with gills, skin, and gut (Fig. 1C), indicating an undiscovered mucosal immune function of the trout PM. Interestingly, although PM is not aggregated into one branch with the gut, the expression patterns of those genes in the PM particularly resembles the gut when compared with the other tissues. Subsequently, we analyzed the abundance of two main B cell subsets (IgM^+ and IgT^+ B cells) in the trout PM and head kidney by flow cytometry (Fig. 1D). Our results showed that the IgT^+ B cells make up ~51.77% of the total B cells in the PM of rainbow trout, whereas ~48.23% of the total B cells are IgM^+ B cells (Fig. 1E). Conversely, the percentage of IgT^+ B cells (~27.23%) in the head kidney of trout was ~3-fold lower than that of IgM^+ B cells (~72.77%) (Fig. 1E). We next analyzed the concentrations of IgT, IgM, and IgD in the pharyngeal mucus and serum and found that the protein concentration of IgM was much higher than those of IgT and IgD in both the pharyngeal mucus and serum (Fig. 1F, 1G). However, the ratio of IgT/IgM and IgD/IgM in the pharyngeal mucus was ~20-fold and ~4-fold higher than those in the serum, respectively (Fig. 1H, 1I), which was similar to that we previously reported in trout nasal and gill mucus (11, 33). To understand the protein characterization of secretory Igs (sIgT, sIgM, and sIgD) in the pharyngeal mucus, we first collected the mucus and then loaded it into a gel filtration column. Similar to what we reported in trout nasal and gill mucus (11, 33), a great portion of IgT in the pharyngeal mucus was present in polymeric form, as it eluted at a fraction similar to that of trout IgM, a tetrameric Ig, but an extremely small portion of IgT was eluted in monomeric form (Supplemental Fig. 1A). Interestingly, immunoblot analysis showed that both the polymeric and monomeric IgT in the pharyngeal mucus migrated in the same position under nonreducing conditions (Supplemental Fig. 1B, right panel), suggesting that the subunits of polymeric IgT are associated by noncovalent interactions. In contrast, mucosal IgM and IgD migrated as a polymer and a monomer, respectively, under the same SDS-PAGE conditions (Supplemental Fig. 1B, left and middle panels).

Trout pharyngeal bacteria are mainly coated with IgT

We previously reported that sIgT plays a dominant role in mucosal immune exclusion by coating a large fraction of microbiota on the mucosal surfaces of trout (31, 33). To test the participation of pharyngeal Igs in immune exclusion, using a previously reported method (32), we isolated the pharyngeal-associated bacteria and measured the levels of coating by trout Igs. Flow cytometry analysis showed that a high proportion of pharyngeal bacteria were stained for IgT (~32%), whereas low proportions were coated with

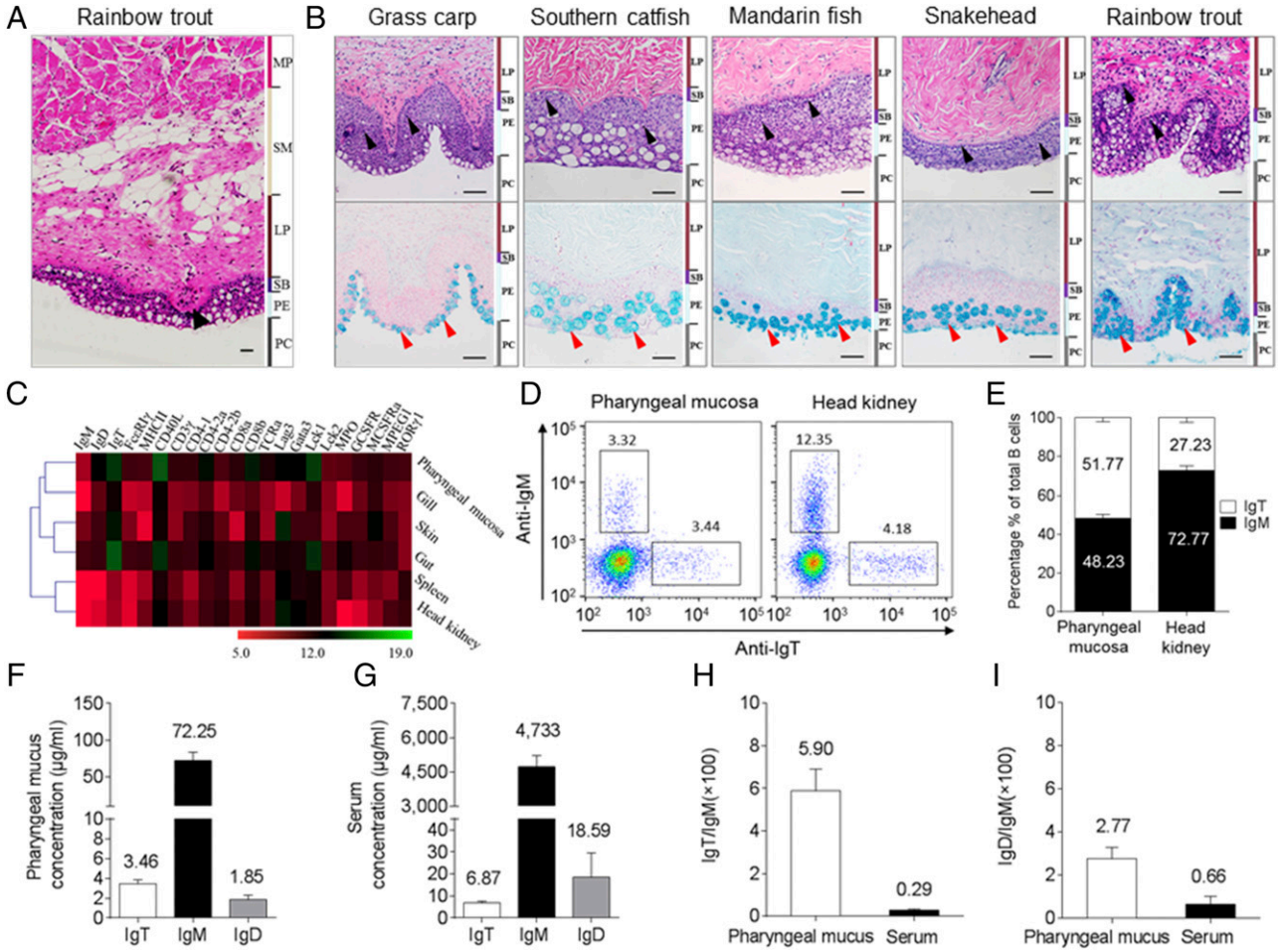

FIGURE 1. General organization of teleost PM lymphoid tissue. (**A**) H&E stain of the pharynx of a control adult rainbow trout (*O. mykiss*). Black arrowhead indicates taste bud. (**B**) H&E (upper) and Alcian blue (lower) stain of the pharynx from five different families of control adult teleost fish. From left to right: grass carp (*C. idellus*), southern catfish (*S. meridionalis*), mandarin fish (*S. chuatsi*), snakehead (*O. argus* Cantor), and rainbow trout (*O. mykiss*). Scale bar, 50 μm. Black and red arrowheads indicate lymphocytes and mucus cells, respectively. (**C**) Heat map illustrates results from qPCR of mRNAs for selected immune markers in trout skin, gut, gill, pharynx, spleen, and head kidney ($n = 6$). Data are expressed as mean cycle threshold (Ct) values ± SEM. (**D**) Flow cytometry analysis of pharynx (left) and head kidney (right) leukocytes stained with anti-IgM and anti-IgT Abs. Numbers in outlined boxes indicate the percentages of IgM^+ (top left) and IgT^+ (bottom right) B cells in the lymphocyte gate, respectively. (**E**) Frequency of IgM^+ and IgT^+ cells among total B cells present in trout pharynx and head kidney. (**F** and **G**) Immunoblot and densitometric analysis of the concentration of IgT, IgM, and IgD in pharyngeal mucus (F) and serum (G). (**H** and **I**) Ratio of IgT to IgM concentration (H) and IgD to IgM concentration (I) in pharyngeal mucus and serum, calculated from the values shown in (F) and (G), respectively. Results in (E)–(I) are expressed as mean ± SEM obtained from 12 individual fishes. MP, muscularis propria; PE, pharyngeal epithelium; SB, stratum basale; SM, submucosa.

IgM (~12%) and IgD (~7%) (Fig. 2A, 2B). Interestingly, these results were similar to previous findings in trout skin (~38% coated with IgT and ~12% with IgM) (32). Moreover, immunoblot analysis showed that more than 50% of the IgT present in the pharyngeal mucus was used for bacteria coating, whereas only 17% of pharyngeal mucosal IgM, and only ~14% of IgD were being used for that purpose (Fig. 2C, 2D). Importantly, using immunofluorescence microscopy, we further confirmed that a high percentage of trout pharyngeal bacteria were coated with mucosal IgT, and a much smaller percentage of bacteria were stained with IgM or IgD (Fig. 2E; isotype-matched control Abs, Supplemental Fig. 2A).

Trout PM elicits strong immune responses to I. multifiliis *parasite infection*

To evaluate the trout PM immune responses to pathogenic challenge, we selected the *I. multifiliis* parasite bath infection model, as it can elicit strong mucosal immune responses in teleosts (42, 43). At 14 d postinfection, the phenotype of small white dots appeared on the trout's skin, gills, and pharyngeal surface (Supplemental Fig. 3B), and a pathological examination and immunofluorescence analysis showed that *I. multifiliis* had successfully invaded the trout PM (Supplemental Fig. 3C). Moreover, by qPCR, we detected the high expression of *I. multifiliis*/18S rRNA in the PM, gills, nose, and skin (Supplemental Fig. 3D). Interestingly, an increased expression trend (peaked on day 28) of *I. multifiliis* parasites in the trout PM was observed postinfection (Supplemental Fig. 3E). We next measured the expression of 19 immune-related genes and cell markers in the PM of trout by qPCR after *I. multifiliis* infection (primers used are shown in Supplemental Table I). Importantly, these results indicated that strong immune responses had occurred in the PM (Fig. 3A). Moreover, in agreement with the pathological changes in the PM (Supplemental Fig. 3A), days 14 and 28 were the most relevant in terms of the intensity of the immune response, and therefore, both were selected for subsequent RNA-Seq analysis. A total of 3909 (day 14) and 5379 (day 28) genes showed significantly differential expression, with 1790 and 2116 genes upregulated and 2119 and 3263 genes downregulated

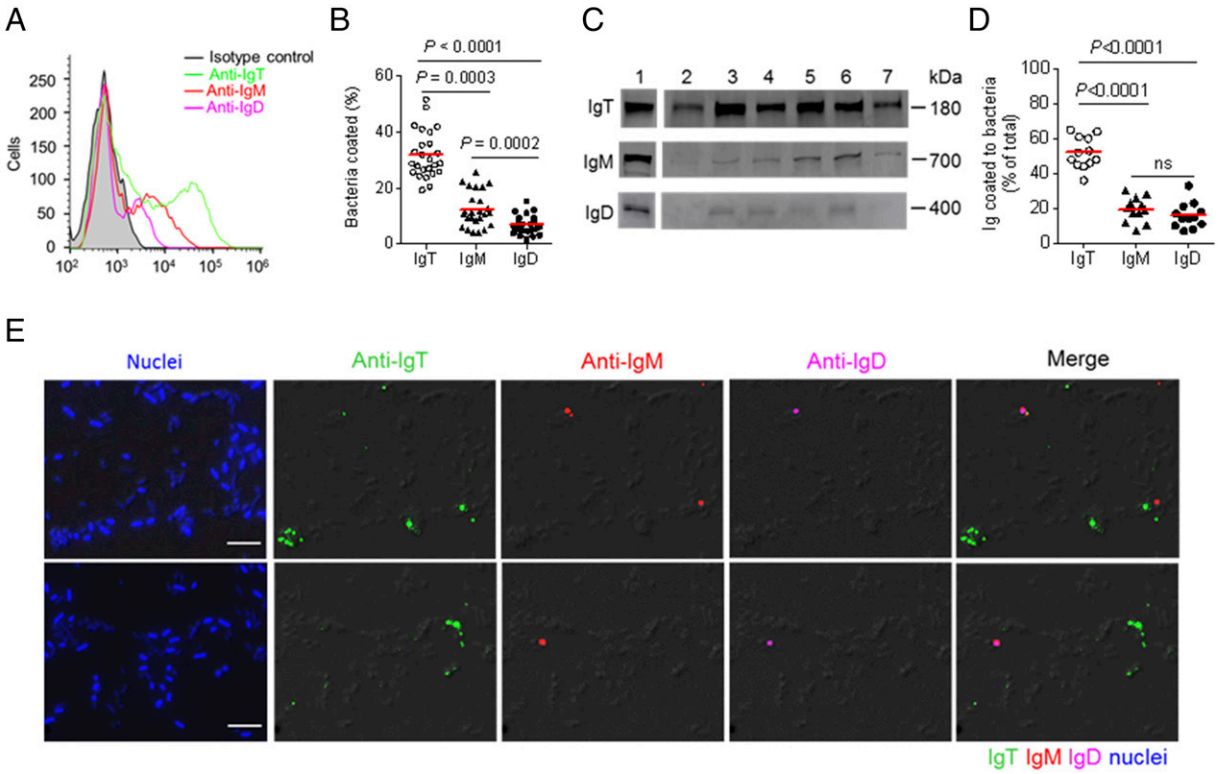

FIGURE 2. A majority of trout pharyngeal bacteria are predominantly coated with IgT. (**A**) Representative flow cytometry histograms showing the staining of pharyngeal bacteria with IgT, IgM, and IgD. Bacteria were stained with isotype controls (shaded histograms), anti-trout IgT (green line), anti-trout IgM (red line), or anti-trout IgD (magenta line) mAbs, respectively. (**B**) Percentages of pharyngeal bacteria coated with IgT, IgM, or IgD ($n = 25$). The median percentage is showed by a red line. (**C**) Immunoblot analysis of IgT, IgM, or IgD coating on pharyngeal bacteria. Lane 1, 0.1 μg of purified IgT, IgM, or IgD; lanes 2–7, pharyngeal bacteria ($n = 6$). (**D**) Percentages of total pharyngeal mucus IgT, IgM, or IgD coating pharyngeal bacteria ($n = 12$). The median is shown by a red line. The statistical differences in (B) and (D) were evaluated by one-way ANOVA with Bonferroni correction. Data are representative of at least three independent experiments. (**E**) Differential interference contrast (DIC) images of pharyngeal bacteria stained with a DAPI/Hoechst solution (blue), anti-IgT (green), anti-IgM (red), or anti-IgD (magenta) and merging IgT, IgM, and IgD staining (Merge) (isotype-matched control Ab staining, Supplemental Fig. 2A). Scale bar, 5 μm.

on days 14 and 28, respectively (Fig. 3B). Importantly, the resulting DEGs were subsequently filtered by the *O. mykiss* immune gene library, and more than 25% of DEGs were identified as immune-related genes, as shown in the pie charts (Fig. 3C, 3D). To further understand the transcriptomic data, we carried out gene ontology enrichment analysis to determine the biological processes that were significantly upregulated in the trout PM after *I. multifiliis* parasite infection. This overview indicated that biological processes representing genes were involved in protein metabolic process, immune system process, response to stress and cytokines, and protein ubiquitination (Fig. 3E, 3F). Importantly, we found on days 14 and 28 a significant modification in the expression of genes involved in 1) innate immunity (Fig. 3G; such as ILs, chemokines, complement factors, antimicrobial peptides, and TLR) and 2) adaptive immunity (Fig. 3H; including Ag-processing and presentation, BCR, and Igs). To validate the RNA-Seq results, 13 DEGs (10 that were upregulated and three that were downregulated) were detected by qPCR, and the results were significantly correlated with the RNA-Seq results at each time point (correlation coefficient $R = 0.91$, $p < 0.001$) (Fig. 3I).

Ig and B cell responses in PM to I. multifiliis *parasite infection*

Using immunofluorescence microscopy, we detected that few IgT^+ and IgM^+ B cells permeated the PM of control fish (Fig. 4A; isotype-matched control Abs, Supplemental Fig. 2B). Interestingly, a moderate increase of IgT^+ B cells was observed in the pharyngeal epithelium of 28-d-infected fish, which was ∼5-fold higher when compared with control fish (Fig. 4B, 4E). Notably, a large accumulation of IgT^+ B cells was found in the pharyngeal epithelium of survivor fish (75 d postinfection), which was ∼6-fold higher when compared with those of control fish (Fig. 4C, 4E). It is worth mentioning that several of these IgT^+ B cells were noticed to be secreting IgT (Fig. 4D, white arrows). In contrast, there was no significant difference in the number of IgM^+ B cells in the infected and survivor fish when compared with that of control fish (Fig. 4A–C, 4E). In agreement with the increase of IgT^+ B cells observed in the PM of infected and survivor fish, the IgT concentration in the pharyngeal mucus of the same fish groups was ∼3-fold and ∼5-fold higher, respectively, when compared with those of control fish (Fig. 4F). However, the protein concentration of IgM and IgD in the pharyngeal mucus remained unchanged after *I. multifiliis* parasite infection (Fig. 4F). Conversely, the IgM concentration was ∼4-fold higher in the serum of both infected and survivor fish when compared with control fish. The concentration of serum IgT was ∼2-fold and ∼3-fold higher in the infected and survivor groups, respectively (Fig. 4G). In contrast, the concentration of IgD remained unchanged in both the pharyngeal mucus and serum of the same fish (Fig. 4F, 4G).

Pathogen-specific Ig responses in PM

The accumulation of IgT^+ B cells and the increase of IgT protein levels in the PM following *I. multifiliis* infection led us to hypothesize a key role of IgT in PM mucosal immunity. To verify this hypothesis, using immunofluorescence microscopy with anti–*I. multifiliis*

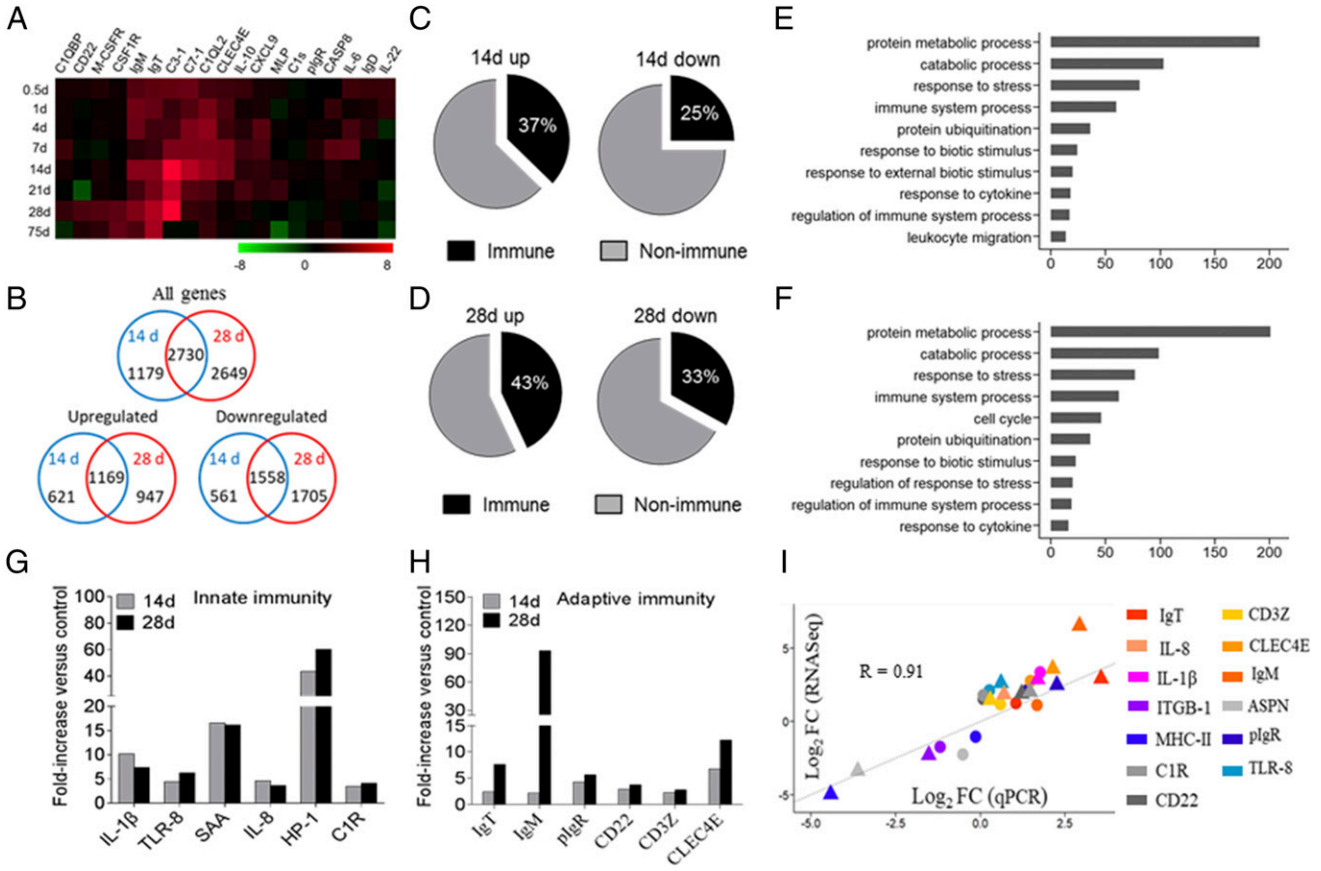

FIGURE 3. Kinetics of the immune response in trout pharynx following *I. multifiliis* parasites infection. (**A**) Heat map demonstrated results from qPCR of mRNAs for selected immune markers in *I. multifiliis*–infected fish versus control fish measured on days 0.5, 1, 4, 7, 14, 21, 28, and 75 postinfection in pharynx of rainbow trout (n = 9). Color value, $\log_2$ (fold change). (**B**) Venn diagrams of RNA-Seq experiment showed the overlap of genes upregulated or downregulated in the pharynx of rainbow trout at 14 or 28 d postinfection with *I. multifiliis* versus control fish (n = 9 per group). (**C** and **D**) Pie charts showed the percentages of immune and nonimmune genes upregulated or downregulated in the pharynx of rainbow trout at 14 (C) and 28 d (D) postinfection with *I. multifiliis* versus control fish by RNA-Seq studies. (**E** and **F**) Biological processes that were significantly altered of rainbow trout 14 (E) and 28 d (F) postinfection with *I. multifiliis* versus control fish revealed by RNA-Seq studies. Fold change differences between control and *I. multifiliis*–infected samples were calculated using cutoff of 2-fold. Significant differential expression at each time point (14 and 28 d) was established by unpaired t tests ($p < 0.05$). (**G** and **H**) Representative innate (G) and adaptive (H) immune genes modulated by *I. multifiliis* infection on day 14 or 28. (**I**) Confirmation of RNA-Seq studies by qPCR of 14 and 28 d infection with *I. multifiliis*. Circle, day 14 after infected with *I. multifiliis*; triangle, day 28 after infected with *I. multifiliis*; rectangle with colors, different colors represent different genes. The selected genes were the following: IgT, IgM, pIgR, Complement C1R (C1R), IL-8, IL-1β, integrin β-1 (ITGB1), MHC (MHC class II), CD22, CD3Z, C-type Lectin Domain Family 4 Member E (CLC4E), asporin (ASPN), and TLR-8.

Ab, *I. multifiliis* trophonts were easily observed in the trout PM 28 d postinfection (Fig. 5A, 5B; isotype-matched control Abs, Supplemental Fig. 2C). Strikingly, most pharyngeal parasites were predominantly coated with IgT, whereas only a few parasites were slightly coated with IgM, and almost no parasites were coated with IgD (Fig. 5A, 5B). Moreover, by a pull-down assay, we measured the capacity of pharyngeal Igs to bind the *I. multifiliis* parasite. Immunoblot analysis showed significant increases of parasite-specific IgT binding in up to 1:10 (~3.1-fold) and 1:40 (~3.5-fold) of the diluted pharyngeal mucus from infected (Fig. 5C, 5G) and survivor fish (Fig. 5D, 5H), respectively, when compared with that of control fish. However, we only found parasite-specific IgM binding in up to a 1:10 (~5.2-fold) pharyngeal mucus dilution from survivor fish (Fig. 5D, 5H), whereas in serum, parasite-specific IgM binding in up to 1:1000 and 1:4000 serum dilutions from infected (Fig. 5E, 5I) and survivor fish (Fig. 5F, 5J) increased by ~3.6-fold and ~4.3-fold, respectively. In contrast, parasite-specific IgT binding was detected only in a 1:10 (~3.8-fold) serum dilution of the survivor fish (Fig. 5E, 5F, 5I, 5J). Interestingly, no parasite-specific IgD binding was detected in either the pharyngeal mucus or serum from infected and survivor fish (Fig. 5C–J).

Local proliferation of B cell and Ig responses in trout PM after I. multifiliis *parasite infection*

To determine whether the substantial increase of IgT^+ B cells in the PM of survivor fish was derived from the process of local IgT^+ B cell proliferation or the transportation of B cells from systemic lymphoid organs, we assessed the in vivo proliferative responses of IgT^+ and IgM^+ B cells from control and survivor fish. Using immunofluorescence microscopy, we detected a significantly higher percentage of EdU^+ IgT^+ B cells (~14.56 ± 2.92% of all IgT^+ B cells) of the PM in survivor fish when compared with that of control fish (~3.69 ± 0.40% of all IgT^+ B cells) (Fig. 6A–C), whereas there was no difference in the proliferation of IgM^+ B cells between control and survivor fish (Fig. 6A–C). Importantly, similar results were obtained by flow cytometric analysis (Fig. 6D–F). The percentage of EdU^+ IgT^+ B cells was significantly higher in the PM of survivor fish (~7.43 ± 0.68% of all IgT^+ B cells) when compared with that of control fish

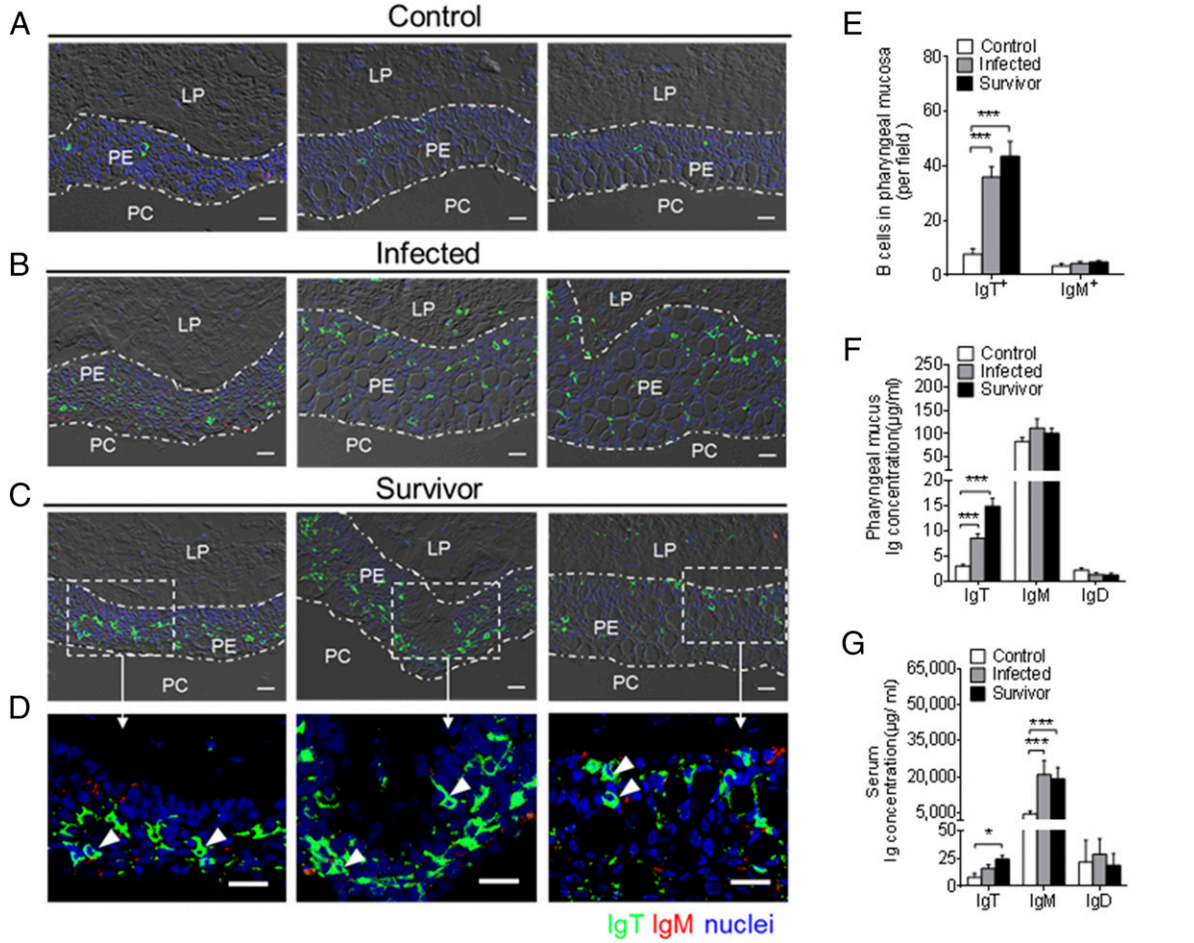

FIGURE 4. Accumulation of IgT$^+$ B cells in the pharynx of trout infected with *I. multifiliis*. (**A**–**C**) Representative differential interference contrast (DIC) images of immunofluorescence staining on paraffinic sections of pharynx from uninfected control fish (A), 28 d–infected fish (B), and survivor fish (C). IgT$^+$ and IgM$^+$ B cells were stained with rabbit anti-trout IgT (green) and mouse anti-trout IgM (red), respectively; nuclei were stained with DAPI (blue) (isotype-matched control Ab staining, Supplemental Fig. 2B). (**D**) Enlarged images of the areas outlined in (C) are showing some IgT$^+$ B cells possibly secreting IgT in pharyngeal epithelium (white arrowhead). Data are representative of at least three independent experiments ($n = 9$ per group). Scale bar, 20 μm. (**E**) Numbers of B cells in control, 28 d–infected, and survivor fish counted from (A)–(C). (**F** and **G**) Concentration of IgT, IgM, and IgD in pharyngeal mucus (F) and serum (G) from uninfected control fish, 28 d–infected fish, and survivor fish ($n = 12$). Data in (E)–(G) are representative of at least three independent experiments (mean ± SEM). *$p < 0.05$, ***$p < 0.001$ (one-way ANOVA with Bonferroni correction). PE, pharyngeal epithelium.

(~3.34 ± 0.39% of all IgT$^+$ B cells) (Fig. 6D–F). However, we found no significant difference in the number of proliferated IgM$^+$ B cells in the trout PM (Fig. 6D–F). In the head kidney, we found an ~2-fold higher number of EdU$^+$ IgM$^+$ B cells in survivor fish (~19.11 ± 1.84% of all IgM$^+$ B cells) when compared with that of control fish (~10.16 ± 0.92% of all IgT$^+$ B cells), whereas no differences in proliferating IgT$^+$ B cells were detected between control and survivor fish (Fig. 6G–I). Therefore, a certain percentage of IgT$^+$ B cells are locally proliferated. To verify whether parasite-specific IgT in phalangeal mucus is locally synthesized in the PM or originated from systemic lymphoid organs, we further analyzed parasite-specific Ig titers from medium of cultured PM, head kidney, and spleen explants from control and survivor fish (Fig. 7). We detected parasite-specific IgT binding in up to 1:40 diluted medium (~3.6-fold) of cultured PM explants of survivor fish, whereas low parasite-specific IgM titers were detected only at the 1:10 dilution in the same medium (Fig. 7A, 7D). On the contrary, the predominant parasite-specific IgM titers (up to 1:40) were found in the medium of survivor head kidney and spleen explants, and low parasite-specific IgT responses (up to 1:10) were detected in the same medium (Fig. 7B, 7C, 7E, 7F). Interestingly, we could not detect any parasite-specific IgD titers in the medium of cultured PM, head kidney, or spleen explants from control and survivor fish (Fig. 7A–F).

pIgR in PM of trout

In mammals, sIgA is transported to PM surfaces mediated by the pIgR (8). Interestingly, previous studies showed that the secretory component of pIgR (tSC) is associated with IgT in the different mucosa of teleosts (18, 31–33). In the current study, using immunoblot analysis under reducing conditions, tSC was detected in the pharyngeal mucus, but not in the serum (Fig. 8A). To determine whether tSC (tpIgR) was associated with pharyngeal mucus IgT, we performed coimmunoprecipitation assays in pharyngeal mucus using Abs against tSC and trout IgT. We found that Abs against trout IgT were able to coimmunoprecipitate pIgR in the pharyngeal mucus (Fig. 8B) and that sIgT in the pharyngeal mucus could be immunoprecipitated by the anti-pIgR Ab (Fig. 8C). Moreover, immunofluorescence microscopy analysis showed that most of pIgR-containing cells were located in the pharyngeal epithelium of trout, and some of those pIgR-containing cells were stained with IgT (Fig. 8D, 8E; isotype-matched control Abs, Supplemental Fig. 2D). It is worth mentioning that a notable accumulation of pIgR-containing cells was observed in the PM

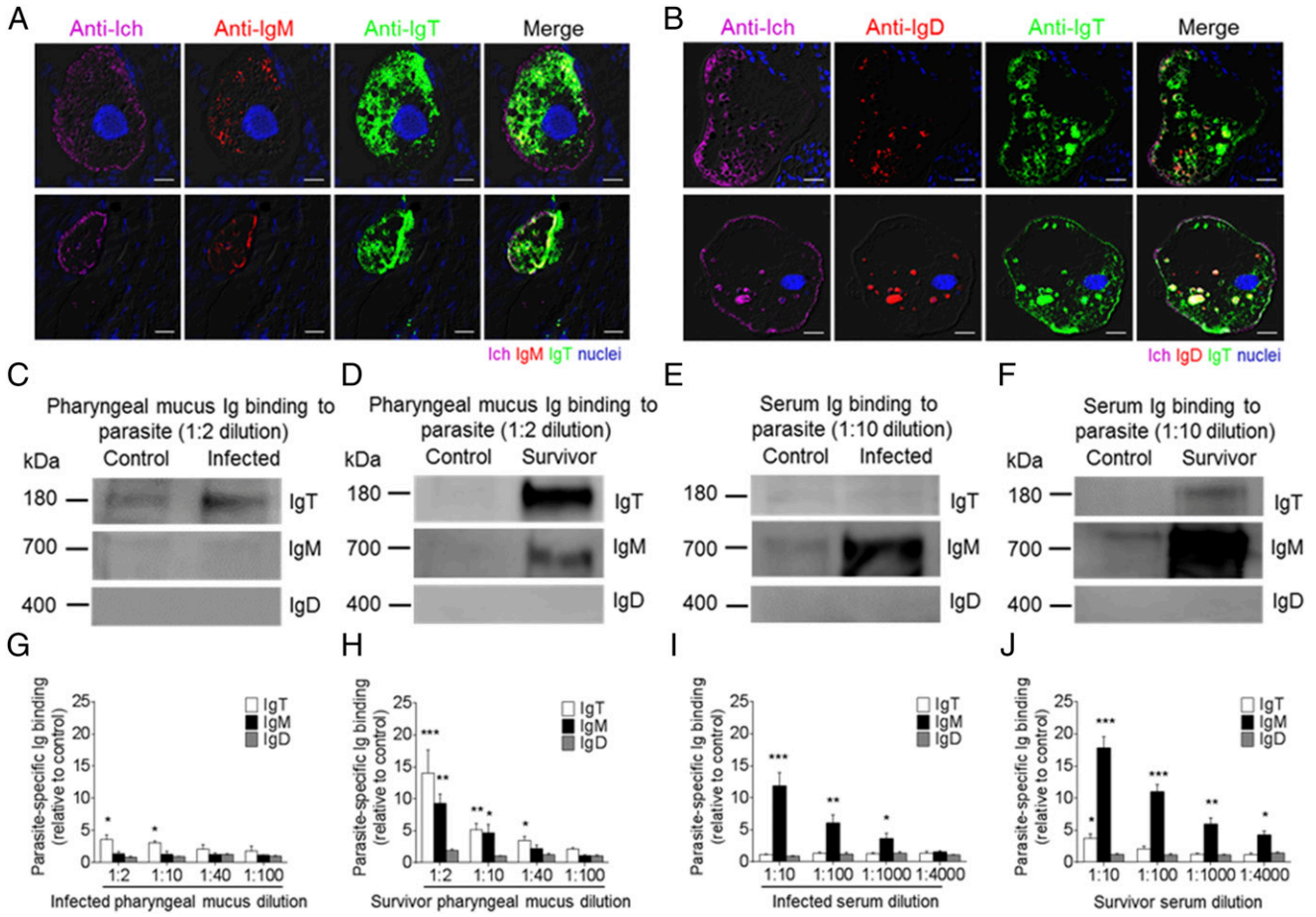

FIGURE 5. Ig-specific responses in the pharynx from infected and survivor fish. (**A** and **B**) Four different microscope images of slides showing immunofluorescence staining of *I. multifiliis* parasites in pharyngeal paraffinic sections from trout infected with *I. multifiliis* after 28 d ($n = 6$). (A) From left to right: *I. multifiliis* (magenta), IgM (red), and IgT (green), with nuclei stained with DAPI (blue). (B) From left to right: *I. multifiliis* (magenta), IgD (red), and IgT (green), with nuclei stained with DAPI (blue); differential interference contrast (DIC) images showing merged staining (isotype-matched control Ab staining, Supplemental Fig. 2C). Scale bar, 20 μm. (**C** and **D**) Western blot analysis of IgT-, IgM-, and IgD-specific binding to *I. multifiliis* in pharyngeal mucus (dilution 1:2) from 28 d–infected (C) and survivor (D) fish. (**E** and **F**) Western blot analysis of IgT-, IgM-, and IgD-specific binding to *I. multifiliis* in serum (dilution 1:10) from 28 d–infected (E) and survivor (F) fish. (**G** and **H**) IgT-, IgM-, and IgD-specific binding to *I. multifiliis* in dilutions of pharyngeal mucus from infected (G) and survivor (H) fish, evaluated by densitometric analysis of immunoblots and presented as relative values to those of control uninfected fish ($n = 12$). (**I** and **J**) IgT-, IgM-, and IgD-specific binding to *I. multifiliis* in dilutions of serum from 28 d–infected (I) and survivor (J) fish, evaluated by densitometric analysis of immunoblots and presented as relative values to those of control uninfected fish ($n = 12$). Data are representative of at least three independent experiments (mean ± SEM). $^*p < 0.05$, $^{**}p < 0.01$, $^{***}p < 0.001$ (unpaired Student t test).

of infected (~2-fold) and survivor fish (~4-fold) when compared with that of control fish (Fig. 8F, 8G). Critically, a significant increase of the pIgR protein levels was detected in the pharyngeal mucus in both infected (Fig. 8H, 7J) and survivor fish (Figs. 8I, 8J, 9).

Discussion

The mammalian pharynx has evolved tonsils strategically located to generate efficient mucosal immunity to protect the PC against airborne and alimentary Ags (6). However, in the ancient bony vertebrates like teleost fish, which lack tonsils in pharynx, whether they have pharyngeal immunity against waterborne Ags remains unknown. In this study, we showed the role of B cell and Ig responses in controlling pathogens in the PC of rainbow trout (*O. mykiss*), presenting molecular mechanisms for mucosal adaptive immunity similar to those within mammals. Thus, our findings revealed that the pharynx serves universally conserved immune defense functions in both primitive and modern bony vertebrates.

In this study, we showed for the first time, to our knowledge, that the trout PM contains diffuse MALT but lacks the organized lymphoid structures (i.e., tonsils), as well as a preponderance of IgT^+ over IgM^+ B cells. Interestingly, IgA^+ B cells are fewer in number than IgG^+ B cells in mammals (44), whereas IgA is the predominant Ig in the nasopharyngeal secretions of infants at 7 wk of age (45). In this study, the protein levels of pharyngeal mucus sIgT were found to be higher than those reported in the skin (~11-fold) (32), gill (2-fold) (33), and nasal mucus (~2-fold) (18) and comparable to those in the gut mucus (31). In line with the case of mammalian sIgA (46–48), IgT protein levels vary at individual mucosal surfaces in fish. Moreover, trout Ig protein characteristic analysis showed that most of the sIgT presents in the pharyngeal mucus as a polymer, similar to the characteristic of sIgA in the respiratory and gastrointestinal tract mucosal surfaces from humans (49). Unlike tetrameric IgM (31), the monomeric subunits of polymeric IgT are associated by noncovalent interactions, as previously found in other sources of mucus in teleosts (18, 31–33). Thus, the predominance of IgT^+ B cells and the higher protein levels of IgT in the pharyngeal mucus suggest a possible role of IgT in pharynx mucosal immunity.

In mammals, sIgA acts as the first line of mucosal defense against microbiota by immune exclusion (50, 51). It has been

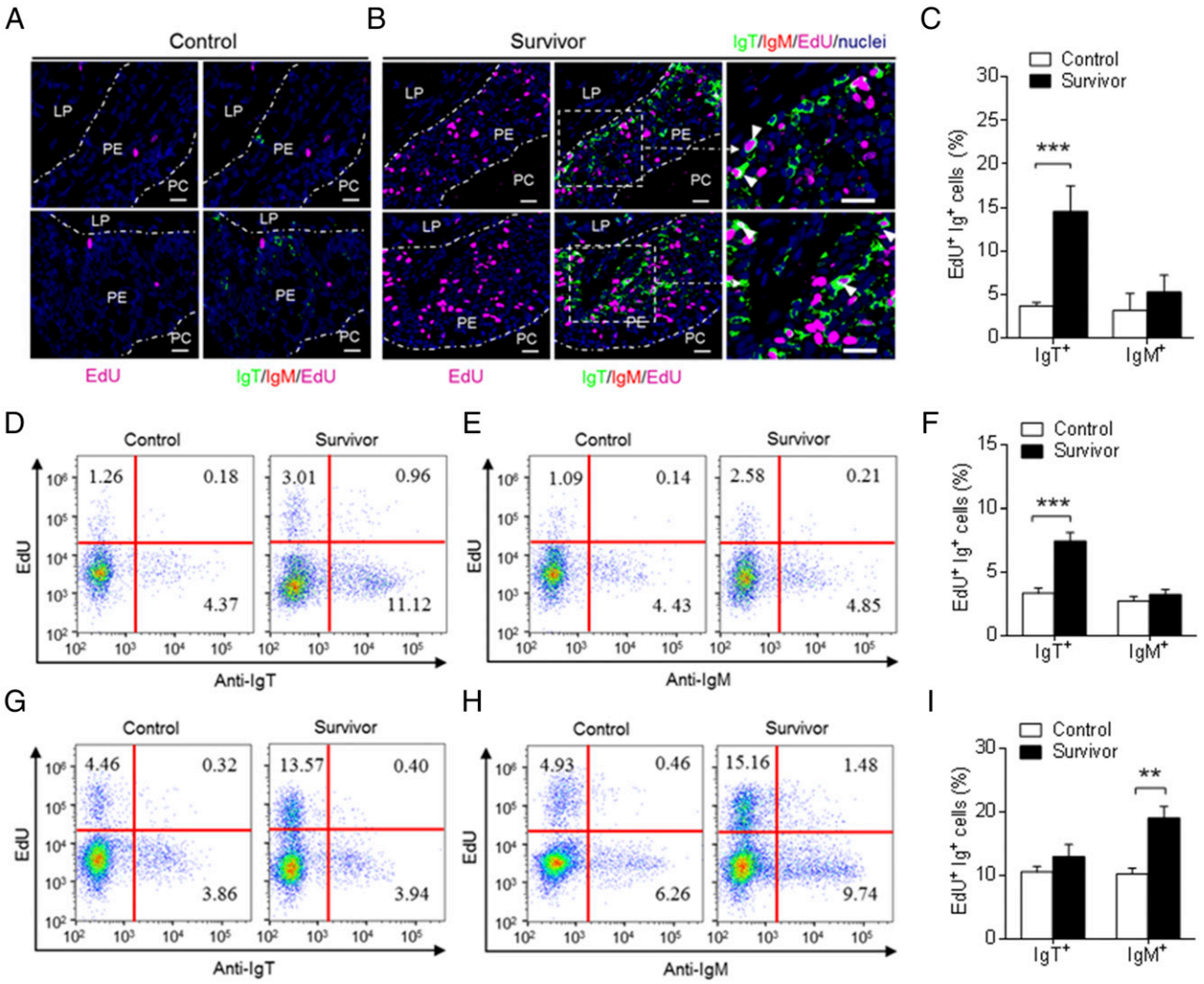

FIGURE 6. Proliferative responses of IgT^+ and IgM^+ B cells in the pharynx of survived fish. (**A** and **B**) Immunofluorescence analysis of EdU incorporation by IgT^+ or IgM^+ B cells in the pharynx of control (A) and survivor fish (B). Pharynx paraffinic sections were stained for EdU (magenta), trout IgT (green), trout IgM (red), and nuclei (blue) detection ($n = 9$). White rectangle represents partial enlargement area. White arrowheads point to cells double stained for EdU and IgT. Data are representative of at least three independent experiments. Scale bar, 20 μm. (**C**) Percentage of EdU^+ cells from the total pharynx IgT^+ or IgM^+ B cell populations in control or survivor fish counted from (A) and (B). (**D** and **E**) Representative flow cytometry dot plot showing proliferation of IgT^+ (D) and IgM^+ (E) B cells in pharynx leukocytes of control and survivor fish. The percentage of lymphocytes representing proliferative B cells (EdU^+) is shown in each dot plot. (**F**) Percentage of EdU^+ cells from the total pharynx IgT^+ or IgM^+ B cell populations in control and survivor fish ($n = 9$). (**G** and **H**) Representative flow cytometry dot plot showing proliferation of IgT^+ (G) and IgM^+ (H) B cells in head kidney leukocytes of control and survivor fish. The percentage of lymphocytes representing proliferative B cells (EdU^+) is shown in each dot plot. (**I**) Percentages of EdU^+ cells from the total head kidney IgT^+ or IgM^+ B cell populations in control and survivor fish ($n = 9$). Data in (C), (F), and (I) are representative of at least three independent experiments (mean ± SEM). $^{**}p < 0.01$, $^{***}p < 0.001$ (unpaired Student t test). PE, pharyngeal epithelium.

estimated that up to 70% of bacteria in the gut lumen are coated with sIgA (less with IgG and IgM) (52), and IgA coating is thought to efficiently inhibit luminal bacteria colonization and invasion of the gut epithelium (53). Our previous findings in trout have shown that, similar to sIgA in mammals, sIgT is the main Ig isotype coating the bacteria in the mucosal surface of fish (18, 31–33). In this study, to our knowledge, we showed for the first time the presence of commensal bacteria in association with the teleost pharyngeal Igs. In the case of trout pharyngeal bacteria, a large population of bacteria was predominantly coated with sIgT and, to a lesser degree, with sIgM and sIgD. Although the PM was thought to be colonized by high densities of microbiota (54, 55), few studies have investigated the relationship between mucosal Igs and PM bacteria. Thus, our results, to our knowledge, provide the first demonstration of the dominant role of mucosal IgT in the control of pharyngeal commensal bacteria in vertebrates. Interestingly, a landmark study demonstrated that the members of the intestinal microbiota (Prevotellaceae, *Helicobacter*, and segmented filamentous bacteria), which are known to preferentially drive intestinal inflammation, are highly coated with IgA (56). In this study, we hypothesize that microbiota species in PM coated with sIgT may have a potential role in triggering inflammatory response. Therefore, future studies need to identify the type of PM microbiota species and address the potential role of PM microbiota species coated with sIgT.

In this study, we report for the first time, to our knowledge, that *I. multifiliis* can invade the trout PM and elicit strong local immune responses. By qPCR, we detected the *I. multifiliis* parasites loads in the trout pharynx began to increase significantly on day 7 postinfection, similar to what we have previously reported in the nose of trout (18). Notably, both innate and adaptive immune molecules are significantly upregulated in the trout PM postinfection.

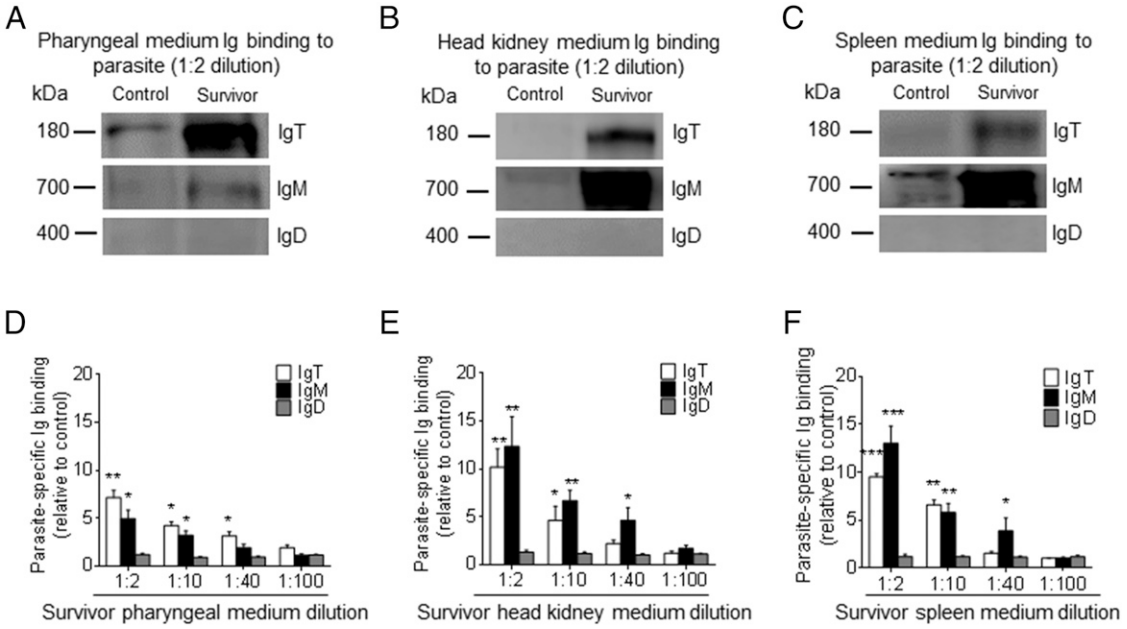

FIGURE 7. Local IgT-, IgM-, and IgD-specific responses to *I. multifiliis* parasite of survivor fish. Pharynx, head kidney, and spleen explants (~30 mg each) from control and survivor fish were cultured in medium (400 μl) for 7 d. (**A**–**C**) Western blot analysis of IgT-, IgM-, and IgD-specific binding to *I. multifiliis* in the culture medium of pharynx (A), head kidney (B), and spleen (C) (dilution 1:2) from control and survivor fish. (**D**–**F**) IgT-, IgM-, and IgD-specific binding to *I. multifiliis* in dilutions of pharynx (D), head kidney (E), and spleen (F) culture medium from survivor fish, evaluated by densitometric analysis of immunoblots and presented as relative values to those of control fish ($n = 12$). Data are representative of at least three independent experiments (mean ± SEM). $*p < 0.05$, $**p < 0.01$, $***p < 0.001$ (unpaired Student t test).

Critically, based on transcriptome sequencing analysis, the upregulated expression of immune-related molecules contains ILs, chemokines, complement factors, antimicrobial peptides, TLR, and Igs known to be crucial in the pharyngeal immune system of mammals (24, 57, 58). Our results concur with the previous studies in which a large number of immune-related genes were upregulated in nasal mucosa from rainbow trout postinfection with *I. multifiliis* parasites (18). Differently, we found that the greatest changes in expression of complement-related genes in nasal mucosa occurred on day 7 postinfection; however, it mainly occurred in PM on day 14 postinfection. In addition, we found that a large accumulation of IgT^+, but not IgM^+, B cells occurred in the pharyngeal epithelium of infected and survivor fish exposed to *I. multifiliis*, in accordance with the increased concentration of IgT, but not IgM or IgD, in the pharyngeal mucus of the same individuals. Similarly, numerous research studies on Ig and plasma cell responses in the mammalian PM have reported on pharyngeal secretions and various tonsils (11, 25, 59). Importantly, higher parasite-specific IgT titers than IgM were detected in the pharyngeal mucus as well as a much higher degree of IgT coating than IgM on the pharyngeal parasites, indicating an important role for sIgT in the control of *I. multifiliis* infection. As expected, we detected an overwhelming prevalence of IgM titers in the serum. Combined, our results support the idea that IgT and IgM responses are specialized in pharyngeal mucosal and systemic immunity, respectively. Interestingly, following intranasal immunization with lipoteichoic acid and cholera toxin B, Ag-specific IgA and IgG responses were evoked effectively in mammal PM and serum, respectively (12, 60). Thus, our results suggest a conserved role of fish sIgT and mammalian sIgA in the protection of the PM from pathogens through convergent evolution.

In mammals, most activated B cells in the PM migrate from tonsillar GCs (6, 8, 58), and the sIgA normally appearing in pharyngeal secretions is produced by local plasma cells that originated from various tonsils (6, 8). However, given the lack of tonsils in teleost fish, it is unclear whether the IgT^+ B cell accumulations originated from local B cell proliferation in the PM or migration from other lymphoid organs. In this study, by in vivo proliferation assays, we showed for the first time, to our knowledge, dominant proliferative IgT^+ B cell responses in the trout PM. In contrast, strong IgM^+ B cell proliferative responses were detected in the head kidney of the same fish. Thus, this finding strongly suggests that the accumulation of IgT^+ B cells in the pharyngeal epithelium is the result of local proliferation rather than migration from the head kidney. Interestingly, similar results were also discovered in the nose and gills (18, 33). In addition, we confirmed the local production of high pathogen-specific IgT titers in PM tissue explant cultures, suggesting the presence of parasite-specific plasma cells in the local PM. Similarly, in the PM from pharyngitis patients, a substantial sIgA seemed to be secreted locally by IgA-secreting plasma cells generated from lymphoid follicles and in the mucosa itself (23). Moreover, by in vitro culture of human tonsil lymphocytes following diphtheria toxoid stimulation, the specific IgA could be measured in the culture supernatant (61). Hence, our data indicate that the local mucosal B cells and secretion of mucosal Ig responses in the PM happen not only in tetrapod species, but also in nontetrapod species such as teleost fish.

To protect the mucosal surfaces from invading pathogens and maintain homeostasis, vertebrates have developed an exquisite mucosal immune system in which the secretory component or the pIgR produced by epithelial cells can transport sIgA to the mucosal surface (8, 62). However, little actual evidence exists in support of the direct interactions between sIgA and pIgR in the PM of vertebrates. Critically, we observed that pIgR-positive cells mainly existed in the epithelial layer of the trout PM, and trout secretory component was associated with sIgT in the pharyngeal mucus. Thus, our finding provides, to our knowledge, the first demonstration that sIgT was transported by pIgR to trout PM. More importantly, following *I. multifiliis* infection, we found a significant increase in the pIgR-positive cells and pIgR

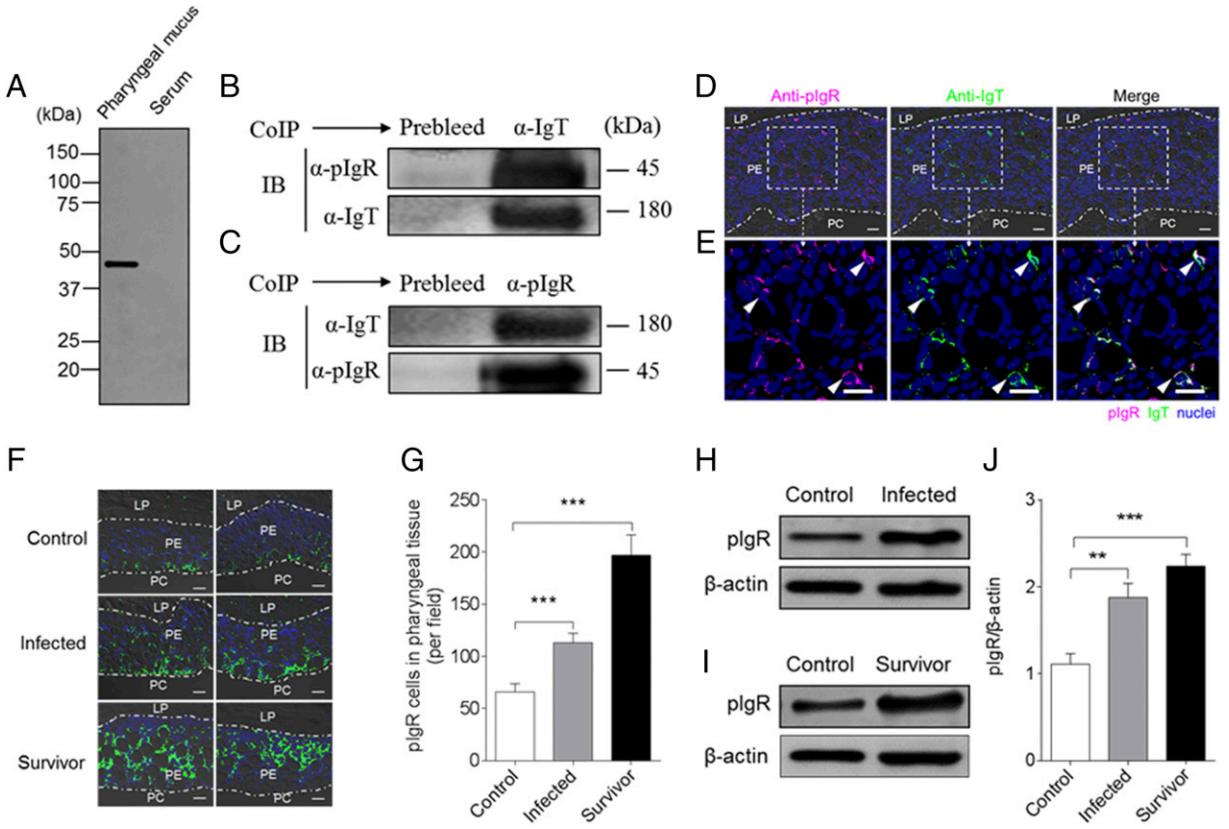

FIGURE 8. Trout pIgR associates with sIgT in pharyngeal mucus. (**A**) SDS-PAGE under reducing conditions of trout pharyngeal mucus and serum, followed by immunoblot analysis (IB) using anti-trout pIgR Ab. (**B**) Coimmunoprecipitation (CoIP) of pharyngeal mucus with rabbit anti-trout IgT Ab, followed by IB under reducing conditions (pIgR detection, upper panels) or nonreducing conditions (IgT detection, lower panels). (**C**) CoIP of pharyngeal mucus with rabbit anti-trout pIgR, followed by (IB) nonreducing conditions (IgT detection, upper panels) or under reducing conditions (pIgR detection, lower panels). IgG purified from rabbit's serum before immunization (Prebleed) served as negative control for rabbit anti-trout IgT and rabbit anti-trout pIgR, respectively [left lane on each panel for (B) and (C)]. (**D**) Immunofluorescence staining for pIgR with IgT in pharynx paraffinic sections of rainbow trout. Differential interference contrast images of pharynx paraffinic sections were stained with anti-trout IgT (green), anti-trout pIgR (magenta), and DAPI for nuclei (blue) ($n = 6$) (isotype-matched control Abs for anti-pIgR in Supplemental Fig. 2D). (**E**) Enlarged sections of the areas outlined in (D) without differential interference contrast (DIC) showing some pIgR/IgT colocalization (white arrowhead). Data are representative of at least three independent experiments. Scale bar, 20 μm. (**F**) Two different DIC images of immunofluorescence staining for pIgR (green) on pharynx paraffinic sections from uninfected control fish (left), infected fish (middle), and survivor fish (right); nuclei are stained with DAPI (blue) ($n = 9$). Data are representative of at least three independent experiments. Scale bar, 20 μm. (**G**) Counts of pIgR cells per field (counted in 27 fields) in paraffinic sections of pharynx from uninfected control fish, infected fish, and survivor fish. (**H**) Representative IB of pIgR (upper panels) in pharyngeal mucus from uninfected control fish (left) and infected fish (right). (**I**) Representative IB of pIgR (upper panels) in pharyngeal mucus from uninfected control fish (left) and survivor fish (right). β-Actin was used as a loading control [lower lane on each panel for (H) and (I)]. (**J**) These data in (H) and (I) were quantified by densitometry, followed by normalization to the β-actin loading control ($n = 9$). Data are representative of at least three independent experiments (mean ± SEM). $^{**}p < 0.01$, $^{***}p < 0.001$ (unpaired Student t test).

protein levels in the PM and pharyngeal mucus, respectively. These results are in agreement with previous findings on human intestinal epithelial cells treated with *Saccharomyces boulardii* and reovirus (63, 64). Moreover, prior studies have shown that pIgR-deficient mice cannot transport polymeric IgA into the intestinal lumen (65). Therefore, to gain insight into the role of pIgR in the homeostasis of PM, future studies are warranted to ascertain the specific contributions of pIgR to the pharyngeal immune responses of teleost fish against pathogens.

In conclusion, our findings indicate the presence of immune function in the PM of teleost fish. To maintain PC homeostasis, fish and mammals have evolved different structures and fascinating strategies in the PM. Mammals have a choana that connects the NC and PC, and their PM is known to contain both mucus glands and mucus-producing cells that produce the mucus that coats their pharyngeal epithelium (20, 21). Importantly, lymphoid structures (i.e., tonsils) are organized in the PM to defense against external pathogens. In that regard, activated IgA^+ B cells generated from GCs migrate into the LP and pharyngeal epithelium, where they are further differentiated into plasmablasts or plasma cells to produce sIgA (6, 8, 58). Subsequently, the sIgA-containing J chain is transported via pIgR-expressing epithelial cells into secretions of PM in control of pathogens (62) (Fig. 9A). In contrast, teleost fish lack the choana and mucus glands, and the PM contains diffuse lymphoid cells without any organized lymphoid tissues. Critically, following pathogenic infection, IgT^+ B cells in the PM epithelium can locally proliferate and differentiate into plasmablasts or plasma cells to produce sIgT and then transport via pIgR-expressing epithelial cells into the outer layer of the PM epithelium in control of pathogens and the recognition of microbiota (Fig. 9B). Thus, different types lymphoid structures (organized versus diffuse) and molecules (sIgA versus sIgT) evolved in PM of mammals and fish, but utilize functionally analogous strategies to maintain PC homeostasis. Overall, these data indicate that the mucosal adaptive immune response in the PM involves a

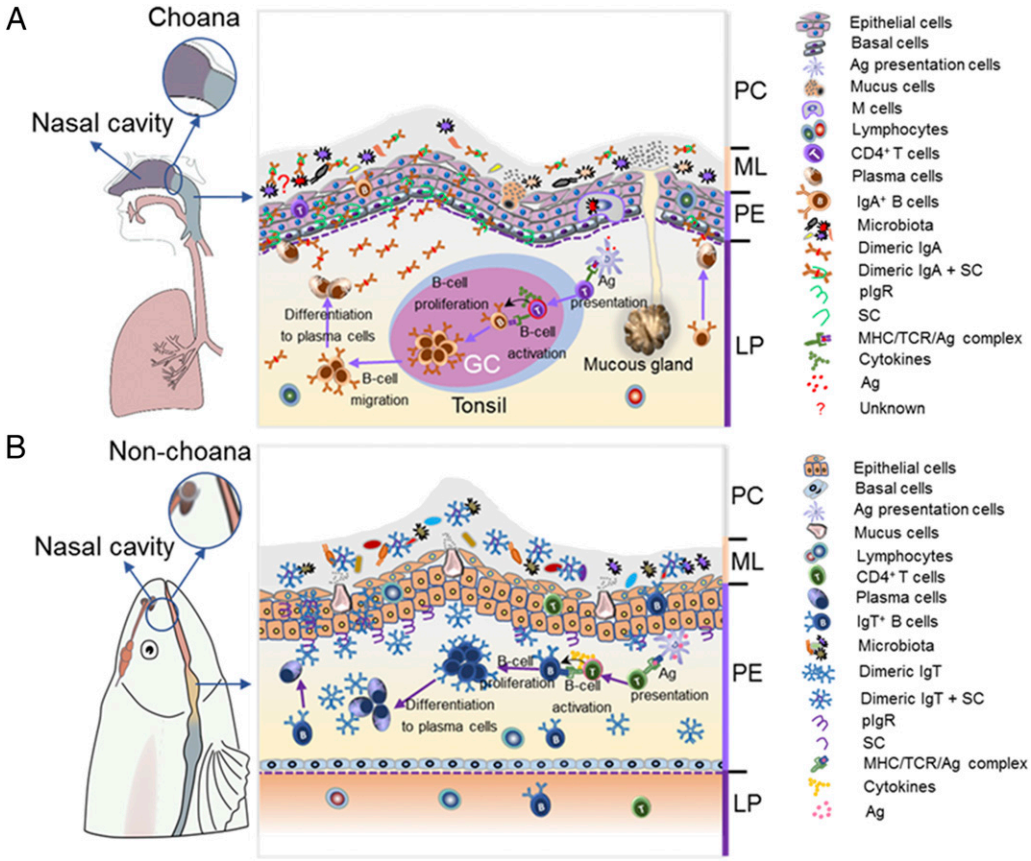

FIGURE 9. Schematic representation of mucosal homeostasis in PM of mammals (**A**) and fish (**B**). (A) Left, In mammals, they have evolved a unique choana that connects the NC and PC, thus forming a passageway to acquire oxygen from external air. (A) Right, All mucosal regions of mammalian PC are covered by PM, which contains two main layers, an outer layer of stratified squamous epithelium (pharyngeal epithelium) and an underlying layer of dense connective tissue (LP). It is populated with both mucus-secreting cells within pharyngeal epithelium (PE) and the mucus gland within LP, which secrete mucus together into mucous layer (ML). Moreover, mammalian PM has organized lymphoid structures (i.e., tonsils) with GC, and upon pathogenic infection, it can generate activated IgA^+ B cells and then migrate into the LP, where they are further differentiated into plasmablasts or plasma cells. Thereafter, IgA containing the joining J chain plasma cells is secreted by plasma cells and transported via pIgR to the ML together with mucus in control of pathogens or the recognition of microbiota. (B) Left, In contrast, because teleost fish lacks the choana, the PC is a separate compartment from the NC. (B) Right, Fish PM has two similar layers, PE and LP. Interestingly, very abundant mucus-secreting cells are instead present, which produce pharyngeal mucus directly into the ML. Moreover, IgT^+ B cells are found scattered mainly in the PE, where they increase in significant numbers upon pathogenic infection. Critically, sIgT is locally generated from these IgT^+ B cells, and it is transported by pIgR produced by parenchymal cells within PE into pharyngeal secretions in control of pathogens or the recognition of microbiota. Overall, in pharyngeal mucosal site, teleost sIgT and mammal sIgA (similar, but slightly different, modes of production) play a conserved role in maintaining PM homeostasis.

process of convergent evolution between tetrapods and nontetrapods.

Acknowledgments

We thank Dr. J. Oriol Sunyer (University of Pennsylvania) for the generous gift of anti-trout IgM, anti-trout IgD, anti-trout IgT mAbs, anti-trout IgT, and anti-trout pIgR pAbs. We thank Dr. Fangkui Wang from the State Key Laboratory of Agricultural Microbiology (Huazhong Agricultural University) for technical help about flow cytometry analysis. We would also like to thank the staff of the Flow Cytometry and Cell Sorting Facility of Wuhan Institute of Biotechnology for immune cell analysis.

Disclosures

The authors have no financial conflicts of interest.

References

1. Graham, A., and J. Richardson. 2012. Developmental and evolutionary origins of the pharyngeal apparatus. *Evodevo* 3: 24.
2. Laitman, J. T., and J. S. Reidenberg. 1993. Specializations of the human upper respiratory and upper digestive systems as seen through comparative and developmental anatomy. *Dysphagia* 8: 318–325.
3. Casteleyn, C., S. Breugelmans, P. Simoens, and W. Van den Broeck. 2011. The tonsils revisited: review of the anatomical localization and histological characteristics of the tonsils of domestic and laboratory animals. *Clin. Dev. Immunol.* 2011: 472460.
4. Janvier, P. 2004. Wandering nostrils. *Nature* 432: 23–24.
5. Zhu, M., and P. E. Ahlberg. 2004. The origin of the internal nostril of tetrapods. *Nature* 432: 94–97.
6. Brandtzaeg, P. 2011. Immune functions of nasopharyngeal lymphoid tissue. *Adv. Otorhinolaryngol.* 72: 20–24.
7. Debertin, A. S., T. Tschernig, H. Tönjes, W. J. Kleemann, H. D. Tröger, and R. Pabst. 2003. Nasal-associated lymphoid tissue (NALT): frequency and localization in young children. *Clin. Exp. Immunol.* 134: 503–507.
8. Perry, M., and A. Whyte. 1998. Immunology of the tonsils. *Immunol. Today* 19: 414–421.
9. Cerutti, A., K. Chen, and A. Chorny. 2011. Immunoglobulin responses at the mucosal interface. *Annu. Rev. Immunol.* 29: 273–293.
10. Sepahi, A., and I. Salinas. 2016. The evolution of nasal immune systems in vertebrates. *Mol. Immunol.* 69: 131–138.
11. Yokoyama, Y., and Y. Harabuchi. 2002. Intranasal immunization with lipoteichoic acid and cholera toxin evokes specific pharyngeal IgA and systemic IgG responses and inhibits streptococcal adherence to pharyngeal epithelial cells in mice. *Int. J. Pediatr. Otorhinolaryngol.* 63: 235–241.
12. Hotomi, M., N. Yamanaka, J. Shimada, M. Suzumoto, Y. Ikeda, A. Sakai, J. Arai, and B. Green. 2002. Intranasal immunization with recombinant outer membrane protein P6 induces specific immune responses against nontypeable *Haemophilus influenzae*. *Int. J. Pediatr. Otorhinolaryngol.* 65: 109–116.
13. Crole, M. R., and J. T. Soley. 2012. Evidence of a true pharyngeal tonsil in birds: a novel lymphoid organ in Dromaius novaehollandiae and Struthio camelus (Palaeognathae). *Front. Zool.* 9: 21.

14. Nickel, R., A. Schummer, and E. Seiferle. 1977. *The Anatomy of the Domestic Birds.* Parey, Berlin, Hamburg.
15. Shields, J. W., D. R. Dickson, W. Abbott, and J. Devlin. 1979. Thymic, bursal and lymphoreticular evolution. *Dev. Comp. Immunol.* 3: 5–22.
16. Tacchi, L., E. T. Larragoite, P. Muñoz, C. T. Amemiya, and I. Salinas. 2015. African lungfish reveal the evolutionary origins of organized mucosal lymphoid tissue in vertebrates. *Curr. Biol.* 25: 2417–2424.
17. Tacchi, L., R. Musharrafieh, E. T. Larragoite, K. Crossey, E. B. Erhardt, S. A. M. Martin, S. E. LaPatra, and I. Salinas. 2014. Nasal immunity is an ancient arm of the mucosal immune system of vertebrates. *Nat. Commun.* 5: 5205.
18. Yu, Y. Y., W. Kong, Y. X. Yin, F. Dong, Z. Y. Huang, G. M. Yin, S. Dong, I. Salinas, Y. A. Zhang, and Z. Xu. 2018. Mucosal immunoglobulins protect the olfactory organ of teleost fish against parasitic infection. *PLoS Pathog.* 14: e1007251.
19. Chatchavalvanich, K., R. Marcos, J. Poonpirom, A. Thongpan, and E. Rocha. 2006. Histology of the digestive tract of the freshwater stingray Himantura signifer compagno and roberts, 1982 (Elasmobranchii, Dasyatidae). *Anat. Embryol. (Berl.)* 211: 507–518.
20. Shimizu, T. 2013. Mucus, goblet cell, submucosal gland. In *Nasal Physiology and Pathophysiology of Nasal Disorders.* Springer, Heidelberg, Germany, p. 1–14.
21. Suzuki, T., T. Sato, M. Kano, and H. Ichikawa. 2013. The distribution of galanin-immunoreactive nerve fibers in the rat pharynx. *Neuropeptides* 47: 231–236.
22. van Kempen, M. J., G. T. Rijkers, and P. B. Van Cauwenberge. 2000. The immune response in adenoids and tonsils. *Int. Arch. Allergy Immunol.* 122: 8–19.
23. Li, Y. 1993. The relationship between SIgA and chronic granular pharyngitis. *J. Laryngol. Otol.* 107: 532–534.
24. Tanaka, N., S. Fukuyama, M. Ushikai, K. Miyashita, and Y. Kurono. 2003. Immune responses of palatine tonsil against bacterial antigens. *Int. Congr. Ser.* 1257: 141–144.
25. Brandtzaeg, P. 2003. Immunology of tonsils and adenoids: everything the ENT surgeon needs to know. [Published erratum appears in 2004 *Int. J. Pediatr. Otorhinolaryngol.* 68: 387.] *Int. J. Pediatr. Otorhinolaryngol.* 67(Suppl. 1): S69–S76.
26. Flajnik, M. F., and M. Kasahara. 2010. Origin and evolution of the adaptive immune system: genetic events and selective pressures. *Nat. Rev. Genet.* 11: 47–59.
27. Salinas, I., Y. A. Zhang, and J. O. Sunyer. 2011. Mucosal immunoglobulins and B cells of teleost fish. *Dev. Comp. Immunol.* 35: 1346–1365.
28. Sunyer, J. O. 2013. Fishing for mammalian paradigms in the teleost immune system. *Nat. Immunol.* 14: 320–326.
29. Edholm, E. S., E. Bengtén, J. L. Stafford, M. Sahoo, E. B. Taylor, N. W. Miller, and M. Wilson. 2010. Identification of two IgD^+ B cell populations in channel catfish, Ictalurus punctatus. *J. Immunol.* 185: 4082–4094.
30. Ramirez-Gomez, F., W. Greene, K. Rego, J. D. Hansen, G. Costa, P. Kataria, and E. S. Bromage. 2012. Discovery and characterization of secretory IgD in rainbow trout: secretory IgD is produced through a novel splicing mechanism. *J. Immunol.* 188: 1341–1349.
31. Zhang, Y. A., I. Salinas, J. Li, D. Parra, S. Bjork, Z. Xu, S. E. LaPatra, J. Bartholomew, and J. O. Sunyer. 2010. IgT, a primitive immunoglobulin class specialized in mucosal immunity. *Nat. Immunol.* 11: 827–835.
32. Xu, Z., D. Parra, D. Gómez, I. Salinas, Y. A. Zhang, L. von Gersdorff Jørgensen, R. D. Heinecke, K. Buchmann, S. LaPatra, and J. O. Sunyer. 2013. Teleost skin, an ancient mucosal surface that elicits gut-like immune responses. *Proc. Natl. Acad. Sci. USA* 110: 13097–13102.
33. Xu, Z., F. Takizawa, D. Parra, D. Gómez, L. von Gersdorff Jørgensen, S. E. LaPatra, and J. O. Sunyer. 2016. Mucosal immunoglobulins at respiratory surfaces mark an ancient association that predates the emergence of tetrapods. *Nat. Commun.* 7: 10728.
34. Pfaffl, M. W. 2001. A new mathematical model for relative quantification in real-time RT-PCR. *Nucleic Acids Res.* 29: e45.
35. Abyzov, A., J. Mariani, D. Palejev, Y. Zhang, M. S. Haney, L. Tomasini, A. F. Ferrandino, L. A. Rosenberg Belmaker, A. Szekely, M. Wilson, et al. 2012. Somatic copy number mosaicism in human skin revealed by induced pluripotent stem cells. *Nature* 492: 438–442.
36. Dobin, A., C. A. Davis, F. Schlesinger, J. Drenkow, C. Zaleski, S. Jha, P. Batut, M. Chaisson, and T. R. Gingeras. 2013. STAR: ultrafast universal RNA-seq aligner. *Bioinformatics* 29: 15–21.
37. Liao, Y., G. K. Smyth, and W. Shi. 2014. FeatureCounts: an efficient general purpose program for assigning sequence reads to genomic features. *Bioinformatics* 30: 923–930.
38. Robinson, M. D., D. J. McCarthy, and G. K. Smyth. 2010. edgeR: a bioconductor package for differential expression analysis of digital gene expression data. *Bioinformatics* 26: 139–140.
39. Wu, J., X. Mao, T. Cai, J. Luo, and L. Wei. 2006. KOBAS server: a web-based platform for automated annotation and pathway identification. *Nucleic Acids Res.* 34: W720–W724.
40. Li, J., D. R. Barreda, Y. A. Zhang, H. Boshra, A. E. Gelman, S. Lapatra, L. Tort, and J. O. Sunyer. 2006. B lymphocytes from early vertebrates have potent phagocytic and microbicidal abilities. *Nat. Immunol.* 7: 1116–1124.
41. Travers, S. P., and K. Nicklas. 1990. Taste bud distribution in the rat pharynx and larynx. *Anat. Rec.* 227: 373–379.
42. Dickerson, H., and T. Clark. 1998. Ichthyophthirius multifiliis: a model of cutaneous infection and immunity in fishes. *Immunol. Rev.* 166: 377–384.
43. Dickerson, H. W., and R. C. Findly. 2014. Immunity to Ichthyophthirius infections in fish: a synopsis. *Dev. Comp. Immunol.* 43: 290–299.
44. Brandtzaeg, P., L. Surjan, Jr., and P. Berdal. 1978. Immunoglobulin systems of human tonsils. I. Control subjects of various ages: quantification of Ig-producing cells, tonsillar morphometry and serum Ig concentrations. *Clin. Exp. Immunol.* 31: 367–381.
45. Taylor, C. E., and G. L. Toms. 1984. Immunoglobulin concentrations in nasopharyngeal secretions. *Arch. Dis. Child.* 59: 48–53.
46. Powell, K. R., R. Shorr, J. D. Cherry, and J. O. Hendley. 1977. Improved method for collection of nasal mucus. *J. Infect. Dis.* 136: 109–111.
47. Okada, T., H. Konishi, M. Ito, H. Nagura, and J. Asai. 1988. Identification of secretory immunoglobulin A in human sweat and sweat glands. *J. Invest. Dermatol.* 90: 648–651.
48. Aufricht, C., W. Tenner, H. R. Salzer, A. E. Khoss, E. Wurst, and K. Herkner. 1992. Salivary IgA concentration is influenced by the saliva collection method. *Eur. J. Clin. Chem. Clin. Biochem.* 30: 81–83.
49. Woof, J. M., and M. W. Russell. 2011. Structure and function relationships in IgA. *Mucosal Immunol.* 4: 590–597.
50. van der Waaij, L. A., P. C. Limburg, G. Mesander, and D. van der Waaij. 1996. In vivo IgA coating of anaerobic bacteria in human faeces. *Gut* 38: 348–354.
51. van Egmond, M., C. A. Damen, A. B. van Spriel, G. Vidarsson, E. van Garderen, and J. G. van de Winkel. 2001. IgA and the IgA Fc receptor. *Trends Immunol.* 22: 205–211.
52. Phalipon, A., A. Cardona, J. P. Kraehenbuhl, L. Edelman, P. J. Sansonetti, and B. Corthésy. 2002. Secretory component: a new role in secretory IgA-mediated immune exclusion in vivo. *Immunity* 17: 107–115.
53. Cerutti, A., and M. Rescigno. 2008. The biology of intestinal immunoglobulin A responses. *Immunity* 28: 740–750.
54. Baltimore, R. S., R. L. Duncan, E. D. Shapiro, and S. C. Edberg. 1989. Epidemiology of pharyngeal colonization of infants with aerobic gram-negative rod bacteria. *J. Clin. Microbiol.* 27: 91–95.
55. Suárez-Arrabal, M. C., C. Mella, S. M. Lopez, N. V. Brown, M. W. Hall, S. Hammond, W. Shiels, J. Groner, M. Marcon, O. Ramilo, and A. Mejias. 2015. Nasopharyngeal bacterial burden and antibiotics: influence on inflammatory markers and disease severity in infants with respiratory syncytial virus bronchiolitis. *J. Infect.* 71: 458–469.
56. Palm, N. W., M. R. de Zoete, T. W. Cullen, N. A. Barry, J. Stefanowski, L. Hao, P. H. Degnan, J. Hu, I. Peter, W. Zhang, et al. 2014. Immunoglobulin A coating identifies colitogenic bacteria in inflammatory bowel disease. *Cell* 158: 1000–1010.
57. Perera, R., P. Tsang, C. Miller, P. Li, M. Lee, and L. Samaranayake. 2011. Identification of differential pharyngeal cytokine profiles during HIV infection. *BMC Proc.* 5(Suppl. 1): P90.
58. Han, Y., Z. J. Bo, M. Y. Xu, N. Sun, and D. H. Liu. 2014. The protective role of TLR3 and TLR9 ligands in human pharyngeal epithelial cells infected with influenza a virus. *Korean J. Physiol. Pharmacol.* 18: 225–231.
59. Kaur, R., T. Kim, J. R. Casey, and M. E. Pichichero. 2012. Antibody in middle ear fluid of children originates predominantly from sera and nasopharyngeal secretions. *Clin. Vaccine Immunol.* 19: 1593–1596.
60. Russell, M. W., Z. Moldoveanu, P. L. White, G. J. Sibert, J. Mestecky, and M. Michalek S. 1996. Salivary, nasal, genital, and systemic antibody responses in monkeys immunized intranasally with a bacterial protein antigen and the Cholera toxin B subunit. *Infect. Immun.* 64: 1272–1283.
61. Platts-Mills, T. A., and K. Ishizaka. 1975. IgA and IgA diphtheria antitoxin responses from human tonsil lymphocytes. *J. Immunol.* 114: 1058–1064.
62. Asano, M., and K. Komiyama. 2011. Polymeric immunoglobulin receptor. *J. Oral Sci.* 53: 147–156.
63. Buts, J. P., P. Bernasconi, J. P. Vaerman, and C. Dive. 1990. Stimulation of secretory IgA and secretory component of immunoglobulins in small intestine of rats treated with Saccharomyces boulardii. *Dig. Dis. Sci.* 35: 251–256.
64. Kaetzel, C. S. 2005. The polymeric immunoglobulin receptor: bridging innate and adaptive immune responses at mucosal surfaces. *Immunol. Rev.* 206: 83–99.
65. Davids, B. J., J. E. Palm, M. P. Housley, J. R. Smith, Y. S. Andersen, M. G. Martin, B. A. Hendrickson, F. E. Johansen, S. G. Svärd, F. D. Gillin, and L. Eckmann. 2006. Polymeric immunoglobulin receptor in intestinal immune defense against the lumen-dwelling protozoan parasite *Giardia. J. Immunol.* 177: 6281–6290.